Electronic Supplementary Material (ESI) for ChemComm.
This journal is © The Royal Society of Chemistry 2019

Supporting Information for:

Fluorescent molecular spring that visualizes the extension and contraction motions of a double-stranded helicate bearing terminal pyrene units triggered by release and binding of alkali metal ions

Daisuke Taura,[ab] Kaori Shimizu,[b] Chiaki Yokota,[b] Riho Ikeda,[a] Yoshimasa Suzuki,[b] Hiroki Iida,[bc] Naoki Ousaka[ab] and Eiji Yashima*[ab]

[a]Department of Molecular and Macromolecular Chemistry, Graduate School of Engineering, Nagoya University, Chikusa-ku, Nagoya 464-8603, Japan.

[b]Department of Molecular Design and Engineering, Graduate School of Engineering, Nagoya University, Chikusa-ku, Nagoya 464-8603, Japan.

[c]Present Address: Department of Chemistry, Graduate School of Natural Science and Technology, Shimane University, 1060 Nishikawatsu, Matsue 690-8504, Japan.

E-mail: yashima@chembio.nagoya-u.ac.jp

Table of Contents

1. Instruments and Materials.

Instruments

The melting points were measured on a Yanaco MP-500D micromelting point apparatus (Yanako, Kyoto, Japan) and were uncorrected. The IR spectra were recorded on a JASCO FT/IR-680 spectrophotometer (JASCO, Tokyo, Japan). The NMR spectra were measured using a Bruker Ascend 500 (Bruker Biospin, Billerica, MA, USA) or a Varian 500AS (Agilent Technologies, Santa Clara, CA, USA) spectrometer operating at 500 MHz for ^{1}H and 125 MHz for ^{13}C using tetramethylsilane (TMS) or a solvent residual peak as the internal standard. The absorption spectra were measured in a 0.1- or 1-cm quartz cell using a JASCO V-570 spectrophotometer. The temperature was controlled with a JASCO ETC-505 apparatus. The fluorescence spectra were measured in a 1-cm quartz cell on a JASCO FP-6500 spectrofluorometer. The electrospray and cold-spray ionization (ESI and CSI) mass spectra were recorded using a JEOL JMS-T100CS mass spectrometer (JEOL, Akishima, Japan). The single crystal X-ray diffraction measurements were performed on a Rigaku Saturn 724+ CCD diffractometer with Mo Kα radiation (λ = 0.71075 Å) at 103 K. The chiral HPLC analyses were performed on a JASCO PU-2080 liquid chromatograph equipped with UV-visible (JASCO MD-2010) and CD (JASCO CD-2095) detectors using a CHIRALPAK IB column (0.46 (i.d.) x 25 cm, Daicel, Osaka, Japan).

Materials

All starting materials were purchased from commercial suppliers and were used without further purification unless otherwise noted. Silica gel (SiO_2) and aminopropyl-modified silica gel (NH-SiO_2) for the flash chromatography were purchased from Merck (Darmstadt, Germany) or Biotage (Charlotte, NC, USA) and Fuji Silysia Chemical Ltd. (Kasugai, Japan), respectively. The dibromo compound (**7**)[S1] and diiodo compound (**10**)[S2] were prepared according to the literature. The dibromo compound (**9**) was prepared according to Scheme S1 being different from the literature.[S2]

2. Synthetic Procedures.

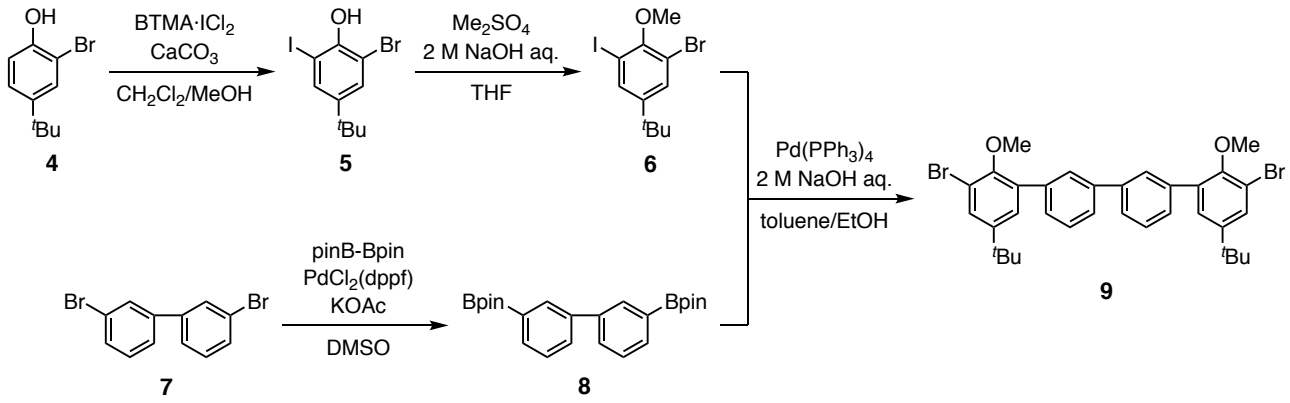

Scheme S1 Synthesis of compound **9**.

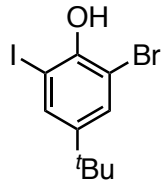

5

5. To a solution of **4** (1.46 g, 6.37 mmol) in $CHCl_3$ (60 mL) and MeOH (24 mL) were added benzyltrimethylammonium dichloroiodate ($BTMA{\cdot}ICl_2$) (2.94 g, 6.71 mmol) and $CaCO_3$ (3.66 g, 6.37 mmol), and the mixture was stirred at room temperature for ca. 8 h under nitrogen. After $BTMA{\cdot}ICl_2$ (0.114 g, 0.328 mmol) was added to this, the mixture was further stirred for 1.5 h. After filtration to remove $CaCO_3$, the solvent was evaporated under reduced pressure. To this was added 5% aqueous $Na_2S_2O_4$ (30 mL) and the mixture was extracted with Et_2O (50 mL × 3). The organic extracts were washed with brine (30 mL) and dried over anhydrous $MgSO_4$. After filtration, the solvent was evaporated under reduced pressure and the residue was purified by column chromatography (SiO_2, *n*-hexane/EtOAc = 40/1 to 20/1 (v/v)) to afford 1.94 g of **5** as a white solid. The purity of **5** was 93% on the basis of its ^{1}H NMR spectrum, and this was subjected to the next step without further purification. A small amount of pure **5** was obtained by flash chromatography (SiO_2, *n*-hexane/EtOAc = 100/0 to 93/7 (v/v) and then *n*-hexane). Mp: 70.7–71.2 °C. IR (KBr, cm^{-1}): 3497, 3469, 2960, 1555, 1476, 1463, 1276, 1164. ^{1}H NMR (500 MHz, $CDCl_3$, 25 °C): δ 7.63 (d, J = 2.2 Hz, 1H, ArH), 7.45 (d, J = 2.2 Hz, 1H, ArH), 5.74 (s, 1H, OH), 1.27 (s, 9H, *t*-Bu). ^{13}C NMR (125 MHz, $CDCl_3$, 25 °C): δ 149.31, 147.02, 135.77, 130.12, 108.23, 83.08, 34.35, 31.41. HRMS (ESI−): *m*/*z* calcd for $C_{10}H_{12}BrIO$ ($M{-}H^+$), 352.9038; found 352.9054.

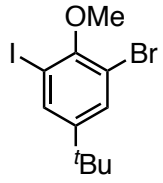

6

6. To a solution of **5** (43.6 g, 123 mmol) in THF (145 mL) were added 2 M aqueous NaOH (30 mL) and dimethyl sulfate (Me_2SO_4) (23.2 mL, 245 mmol), and the mixture was stirred at room temperature for 3 h. After the solvent was evaporated under reduced pressure, the mixture was extracted with EtOAc (400 mL × 3). The organic extracts were washed with brine (400 mL), and dried over anhydrous $MgSO_4$. After filtration, the solvent was evaporated under reduced pressure and the residue was purified by column chromatography (SiO_2, *n*-hexane) to afford 42.0 g of **6** as a white solid. The purity of **6** was 93% on the basis of its ^{1}H NMR spectrum, and this was subjected to the next step without further purification.

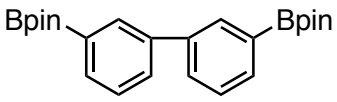

8

8. A mixture of **7** (9.37 g, 30.0 mmol), bis(pinacolato)diboron (pinB-Bpin) (16.8 g, 66.2 mmol), $PdCl_2(dppf)\cdot CH_2Cl_2$ (3.71 g, 4.54 mmol), and KOAc (17.6 g, 180 mmol) in degassed DMSO (200 mL) was stirred at 80 °C for 21 h under nitrogen. After being cooled to room temperature, H_2O (300 mL) was added to this. After filtration using Celite, the mixture was extracted with EtOAc (200 mL × 4). The organic extracts were washed with brine (200 mL), and dried over anhydrous $MgSO_4$. After filtration, the solvent was evaporated under reduced pressure and the residue was purified by column chromatography (SiO_2, *n*-hexane/EtOAc = 10/0 to 10/1 (v/v) and $CHCl_3$) to afford **8** (7.89 g, 64.7% yield) as a white solid. Mp: 163.2–163.8 °C. IR (KBr, cm^{-1}): 2979, 1601, 1475, 1352, 1271, 1212, 1143. ^{1}H NMR (500 MHz, $CDCl_3$, 25 °C): δ 8.06 (bs, 2H, ArH), 7.79 (dt, J = 7.5, 1.2 Hz, 2H, ArH), 7.73–7.70 (m, 2H, ArH), 7.45–7.42 (m, 2H, ArH), 1.37 (s, 24H, $C(CH_3)_2$). ^{13}C NMR (125 MHz, $CDCl_3$, 25 °C): δ 140.70, 133.81, 133.66, 130.44, 128.20, 83.99, 25.03 (7 signals out of 8 expected ones). HRMS (CSI+): *m*/*z* calcd for $C_{24}H_{32}B_2O_4$ ($M+Na^+$), 429.2393; found 429.2397.

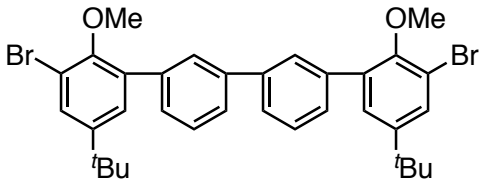

9

9. To a solution of **6** (18.8 g, 51.0 mmol), **8** (10.0 g, 24.6 mmol), and $Pd(PPh_3)_4$ (2.02 g, 1.75 mmol) in degassed toluene (150 mL) and EtOH (150 mL) was added 2 M degassed aqueous Na_2CO_3 (75 mL), and the mixture was stirred at 80 °C for 18 h under nitrogen. After $Pd(PPh_3)_4$ (285 mg, 0.247 mmol) and **6** (227 mg, 0.615 mmol) were added to this, the mixture was further stirred at 80 °C for 6 h. After being cooled to room temperature, H_2O (500 mL) was added to this. The mixture was extracted with $CHCl_3$ (250 mL × 3), and the organic extracts were washed with brine (250 mL) and dried over anhydrous $MgSO_4$. After filtration, the solvent was evaporated under reduced pressure and the residue was purified by column and flash chromatography (SiO_2, *n*-hexane/EtOAc = 1/0 to 30/1 (v/v) and NH-SiO_2, *n*-hexane/EtOAc = 1/0 to 50/1 (v/v)) to afford **9** (8.87 g, 56.5% yield) as a white solid. Spectroscopic data of **9** agreed well with those prepared in a different synthetic route.[S2] The dibromo compound **9** was then converted to the diiodo compound (**10**) according to the procedure reported previously.[S2]

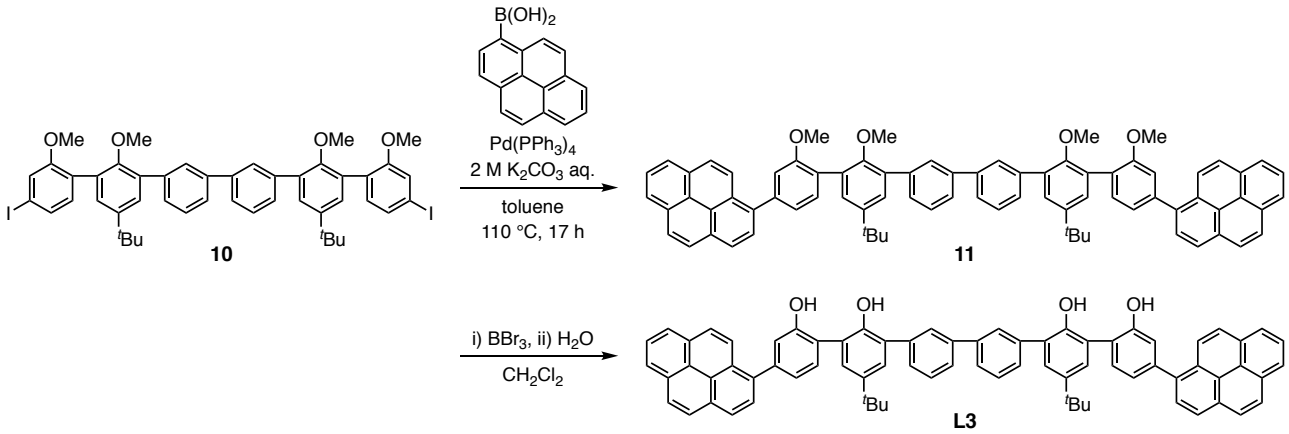

Scheme S2 Synthesis of pyrenyl ligand (**L3**).

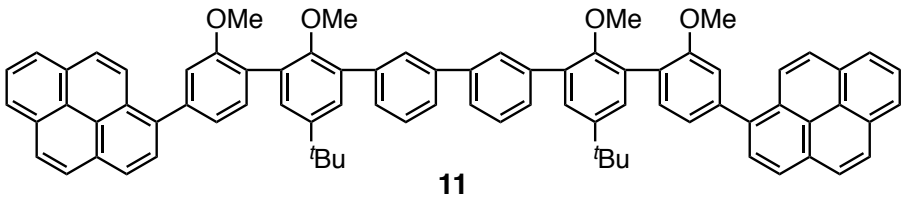

11

11. To a mixture of **10** (141 mg, 0.150 mmol),[S2] 1-pyreneboronic acid (92.3 mg, 0.375 mmol), and $Pd(PPh_3)_4$ (17.3 mg, 0.0150 mmol) in toluene (6.0 mL) was added 2 M aqueous K_2CO_3 (0.75 mL)

and the mixture was stirred at 110 °C for 15.5 h under nitrogen. After being cooled to room temperature, the mixture was extracted with EtOAc (10 mL). The organic extract was washed with H_2O (10 mL × 2) and brine (10 mL × 2), and dried over anhydrous $MgSO_4$. After filtration, the solvent was evaporated under reduced pressure and the residue was purified by flash chromatography (SiO_2, *n*-hexane/EtOAc = 10/0 to 8/2 (v/v)) to afford **11** (139 mg, 84.8% yield) as a yellowish-white solid. Mp: 180.9–182.2 °C. IR (KBr, cm^{-1}): 2959, 1603, 1460, 1227, 1011. ^1H NMR (500 MHz, $CDCl_3$, 25 °C): δ 8.34 (d, J = 9.5 Hz, 2H, ArH), 8.23 (d, J = 8.0 Hz, 2H, ArH), 8.20 (dd, J = 7.5, 0.95 Hz, 2H, ArH), 8.18–8.16 (m, 2H, ArH), 8.10 (s, 4H, ArH), 8.08–8.00 (m, 8H, ArH), 7.70–7.66 (m, 4H, ArH), 7.55 (t, J = 7.5 Hz, 2H, ArH), 7.55 (d, J = 7.5 Hz, 2H, ArH), 7.48–7.46 (m, 4H, ArH), 7.31 (dd, J = 7.5, 1.6 Hz, 2H, ArH), 7.27–7.26 (m, 2H, ArH), 3.88 (s, 6H, OCH_3), 3.39 (s, 6H, OCH_3), 1.43 (s, 18H, *t*-Bu). ^{13}C NMR (125 MHz, $CDCl_3$, 25 °C): δ 156.97, 153.50, 146.20, 141.81, 141.35, 140.23, 137.87, 134.17, 131.72, 131.65, 131.61, 131.14, 130.76, 128.77, 128.68, 128.46, 128.45, 127.84, 127.69, 127.63, 127.59, 127.57, 127.54, 126.17, 126.05, 125.58, 125.27, 125.13, 125.07, 125.00, 124.77, 122.85, 113.60, 60.93, 55.98, 34.70, 31.76 (37 signals out of 38 expected ones). HRMS (ESI+): *m*/*z* calcd for $C_{80}H_{66}O_4$ ($M+Na^+$), 1113.4859; found 1113.4881.

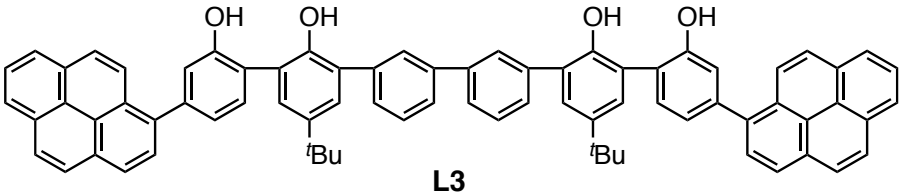

L3

L3. To a solution of **11** (169 mg, 0.155 mmol) in CH_2Cl_2 (5.2 mL) was added a CH_2Cl_2 solution of BBr_3 (1.0 M, 1.55 mL, 1.6 mmol) at –78 °C under nitrogen. After being warmed to room temperature, the mixture was stirred for 7 h. The mixture was then quenched with H_2O (6.8 mL) at 0 °C and further stirred at room temperature for 1 h. After evaporation of the solvent, the aqueous layer was extracted with EtOAc (20 mL, 10 mL × 2). The combined organic layer was washed with 1 M HCl (15 mL), H_2O (15 mL), and brine (15 mL), and dried over anhydrous $MgSO_4$. After filtration, the solvent was evaporated under reduced pressure and the residue was purified by flash chromatography (SiO_2, *n*-hexane/EtOAc = 10/0 to 7/3 (v/v)) to afford **L3** (137 mg, 85.6% yield) as a white solid. Mp: 195.6–197.0 °C. IR (KBr, cm^{-1}): 3528, 2959, 1602, 1459, 1219. ^1H NMR (500 MHz, $CDCl_3$, 25 °C): δ 8.34 (d, J = 9.5 Hz, 2H, ArH), 8.20 (dd, J = 7.5, 0.90 Hz, 2H, ArH), 8.19 (d, J = 8.0 Hz, 2H, ArH), 8.14 (d, J = 7.5 Hz, 2H, ArH), 8.11–8.07 (m, 4H, ArH), 8.04–7.99 (m, 4H, ArH), 7.92 (br s, 2H, ArH), 7.77–7.74 (m, 2H, ArH), 7.67–7.61 (m, 2H, ArH), 7.55 (d, J = 7.5 Hz, 2H, ArH), 7.49 (d, J = 2.5 Hz, 2H, ArH), 7.46 (d, J = 2.5 Hz, 2H, ArH), 7.37–7.35 (m, 2H, ArH),

6.20 (s, 2H, OH), 5.82 (s, 2H, OH), 1.42 (s, 18H, *t*-Bu). ^{13}C NMR (125 MHz, $CDCl_3$, 25 °C): δ 153.42, 147.12, 144.91, 143.02, 141.76, 138.32, 137.03, 131.63, 131.46, 131.14, 130.85, 129.95, 128.71, 128.66, 128.61, 128.58, 127.95, 127.69, 127.65, 127.62, 127.55, 126.98, 126.15, 125.48, 125.28, 125.11, 125.05, 125.03, 124.81, 124.31, 124.05, 124.01, 119.45, 34.64, 31.78 (35 signals out of 36 expected ones). HRMS (ESI−): *m*/*z* calcd for $C_{76}H_{58}O_4$ ($M-H^+$), 1033.4257; found 1033.4231.

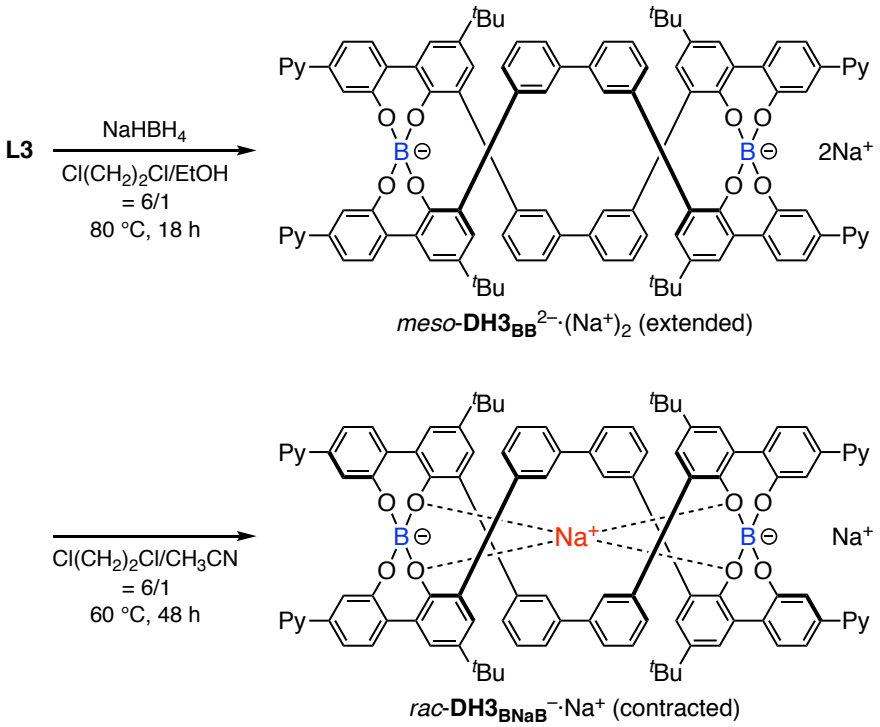

Scheme S3 Synthesis of *meso*- (*meso*-$\mathbf{DH3_{BB}}^{2-}\cdot(Na^+)_2$) and *racemo*-pyrenyl helicates (*rac*-$\mathbf{DH3_{BNaB}}^{-}\cdot Na^+$).

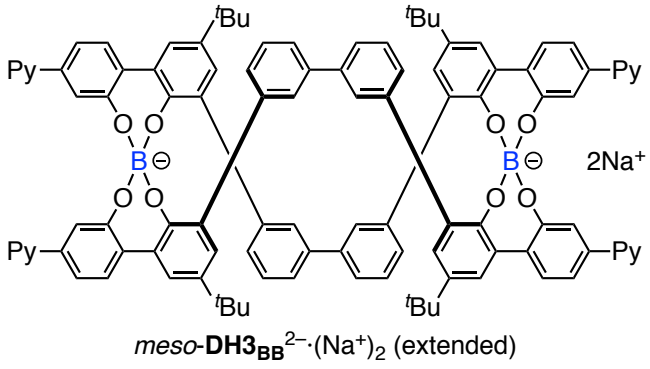

***meso*-$\mathbf{DH3_{BB}}^{2-}\cdot(Na^+)_2$.** To a mixture of **L3** (589 mg, 0.569 mmol) and $NaBH_4$ (21.5 mg, 0.568 mmol) in 1,2-dichloroethane (72 mL) was added EtOH (12 mL) and the reaction mixture was stirred at 80 °C for 18 h under nitrogen. The precipitate obtained from the mixture during the

reaction was collected by filtration, washed with 1,2-dichloroethane, and dried *in vacuo* to afford *meso*-**DH3$_{BB}$**$^{2-}$·(Na$^+$)$_2$ (332 mg, 55.1% yield) as a pale yellow-green solid. Mp: > 300 °C. IR (KBr, cm^{-1}): 2960, 1602, 1459, 989. ^{1}H NMR (500 MHz, CD_3CN, 25 °C): δ 8.36 (d, J = 9.0 Hz, 4H, ArH), 8.12 (d, J = 7.5 Hz, 4H, ArH), 8.05–7.94 (m, 20H, ArH), 7.80 (t, J = 7.5 Hz, 4H, ArH), 7.61 (br s, 8H, ArH), 7.61 (d, J = 7.5 Hz, 4H, ArH), 7.58 (d, J = 2.5 Hz, 4H, ArH), 7.38–7.37 (m, 8H, ArH), 7.37 (d, J = 2.5 Hz, 4H, ArH), 7.23 (dd, J = 7.5, 1.9 Hz, 4H, ArH), 7.15 (br s, 4H, ArH), 6.92 (t, J = 7.5 Hz, 4H, ArH), 1.53 (s, 36H, *t*-Bu). ^{13}C NMR (125 MHz, DMSO-d_6, 25 °C): δ 157.01, 152.26, 140.87, 140.26, 139.93, 139.53, 137.52, 131.51, 131.10, 130.90, 130.26, 130.20, 129.73, 129.64, 129.45, 127.50, 127.42, 127.26, 127.15, 127.10, 126.46, 126.07, 125.71, 125.32, 125.05, 124.90, 124.82, 124.77, 124.56, 124.16, 124.03, 123.75, 123.61, 121.82, 33.94, 31.75. HRMS (ESI−): *m*/*z* calcd for $C_{152}H_{108}B_2Na_2O_8$ (M−2Na$^+$), 1041.4133; found 1041.4116.

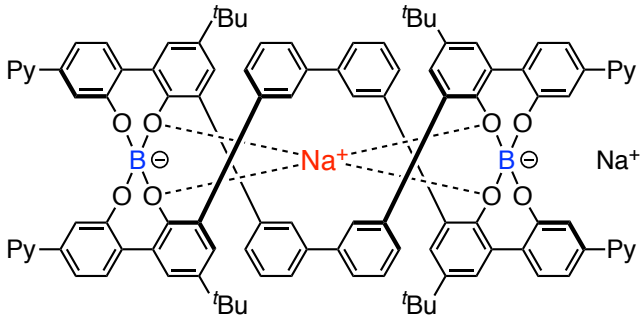

rac-**DH3$_{BNaB}$**$^-$·Na$^+$ (contracted)

***meso*-DH3$_{BB}$$^{2-}$·(Na$^+$)$_2$ to *rac*-DH3$_{BNaB}$$^-$·Na$^+$ Isomerization.** A solution of *meso*-**DH3$_{BB}$**$^{2-}$·(Na$^+$)$_2$ (55.7 mg, 23.4 μmol) in a mixed solvent (1,2-dichloroethane/CH_3CN = 6/1 (v/v)) (35 mL) was stirred at 60 °C for 48 h under nitrogen. After being cooled to room temperature, the solvents were evaporated under reduced pressure. The residue was then purified by precipitation with $CHCl_3$ containing a small amount of EtOH/*n*-hexane (1/1 (v/v)) to afford *rac*-**DH3$_{BNaB}$**$^-$·Na$^+$ (50.8 mg, 91.2% yield) as a white solid that contained a small amount of *meso*-**DH3$_{BB}$**$^{2-}$·(Na$^+$)$_2$ (ca. 1 mol%) as determined by the ^{1}H NMR analysis (see Fig. S1). Mp: > 300 °C. IR (KBr, cm^{-1}): 2960, 1603, 1458, 990. ^{1}H NMR (500 MHz, CD_2Cl_2/CD_3CN = 3/1 (v/v), 25 °C): δ 8.20 (d, J = 7.5 Hz, 4H, ArH), 8.14–8.08 (m, 20H, ArH), 7.99 (t, J = 7.5 Hz, 4H, ArH), 7.85 (d, J = 9.5 Hz, 4H, ArH), 7.54 (d, J = 7.5 Hz, 4H, ArH), 7.47 (s, 4H, ArH), 7.26 (d, J = 2.4 Hz, 4H, ArH), 7.15 (s, 4H, ArH), 7.02 (d, J = 7.5 Hz, 8H, ArH), 6.83 (d, J = 7.5 Hz, 4H, ArH), 6.54 (d, J = 7.5 Hz, 4H, ArH), 6.36 (s, 4H, ArH), 6.26–6.23 (m, 4H, ArH), 1.30 (s, 36H, *t*-Bu). ^{13}C NMR (125 MHz, CD_2Cl_2/CD_3CN = 3/1 (v/v), 25 °C): δ 154.71, 150.16, 143.55, 140.47, 140.16, 139.87, 138.12, 132.81, 131.91, 131.71, 131.21, 130.22, 129.36, 129.23, 128.60, 128.21, 128.11, 128.07, 128.02, 127.80, 127.69, 127.12, 126.94,

126.47, 126.22, 126.06, 125.38, 125.06, 125.00, 124.90, 124.71, 124.64, 123.48, 122.38, 34.15, 31.43. HRMS (ESI−): *m*/*z* calcd for $C_{152}H_{108}B_2Na_2O_8$ ($M-Na^+$), 2105.8164; found 2105.8143.

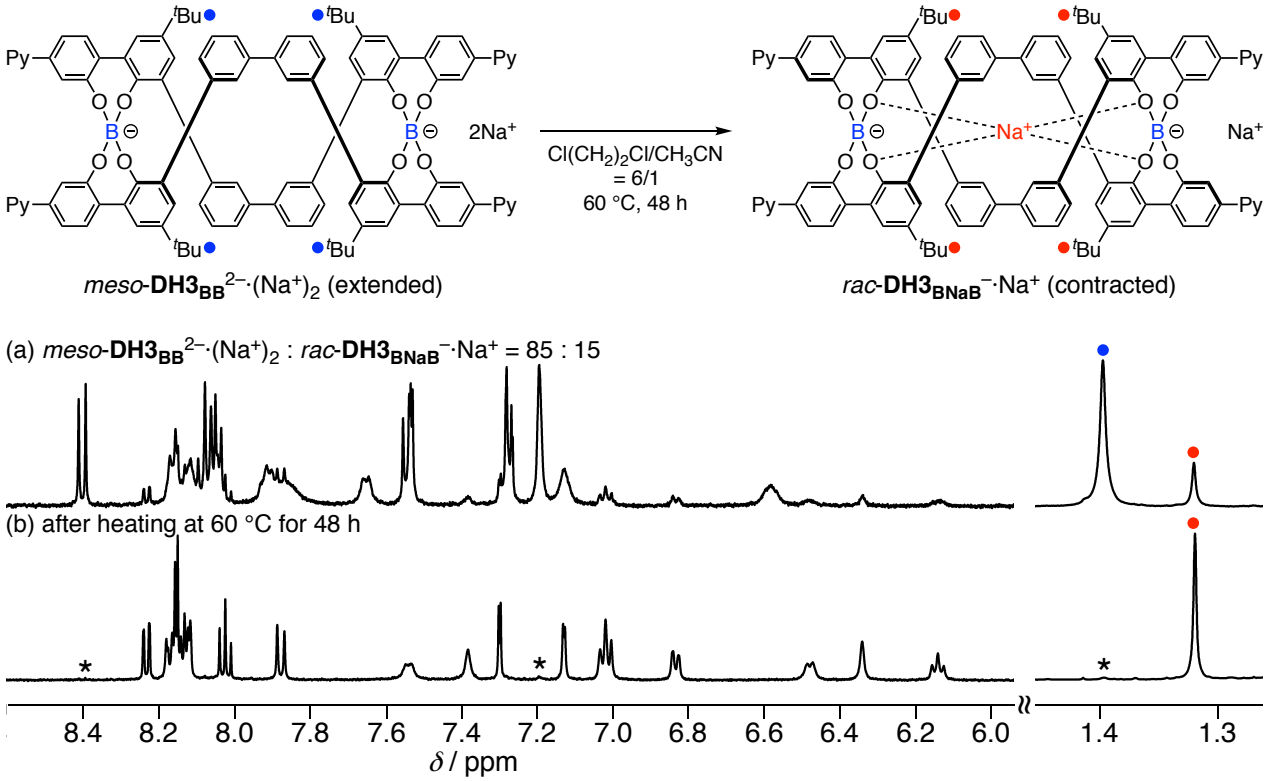

Fig. S1 Partial ^{1}H NMR spectra (500 MHz, CD_2Cl_2/CD_3CN = 6/1 (v/v), 25 °C) of *meso*-$\mathbf{DH3_{BB}}^{2-}$·$(Na^+)_2$ after *meso*-to-*racemo* isomerization (*meso*-$\mathbf{DH3_{BB}}^{2-}$·$(Na^+)_2$/*rac*-$\mathbf{DH3_{BNaB}}^{-}$·Na^+ = 85/15) in CD_2Cl_2/CD_3CN (6/1, (v/v)) (a) and *rac*-$\mathbf{DH3_{BNaB}}^{-}$·Na^+ obtained after heating at 60 °C for 48 h in $Cl(CH_2)_2Cl/CH_3CN$ (6/1 (v/v)). (b) is the same ^{1}H NMR spectrum in Fig. 3a(iii). * denotes the ^{t}Bu and aromatic protons from *meso*-$\mathbf{DH3_{BB}}^{2-}$·$(Na^+)_2$ (ca. 1 mol%).

3. X-ray Crystallographic Data

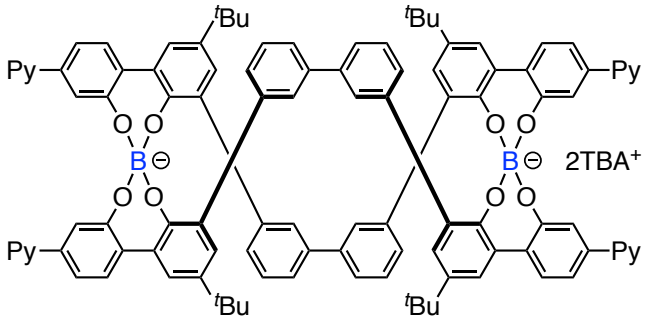

meso-$\mathbf{DH3_{BB}}^{2-}\cdot(TBA^{+})_2$ (extended)

Crystallographic Data of *meso*-$\mathbf{DH3_{BB}}^{2-}\cdot(TBA^{+})_2$

X-ray diffraction data set for *meso*-$\mathbf{DH3_{BB}}^{2-}\cdot(TBA^{+})_2$ was collected on a Rigaku Saturn 724+ CCD diffractometer with Mo Kα radiation (λ = 0.71075 Å) at 103 K. Single crystals of *meso*-$\mathbf{DH3_{BB}}^{2-}\cdot(TBA^{+})_2$ [$C_{200}H_{204}B_2N_{10}O_8$, MW = 2897.35] suitable for X-ray analysis were obtained from an CH_3CN solution of *meso*-$\mathbf{DH3_{BB}}^{2-}\cdot(Na^{+})_2$ (0.50 mM, 0.40 mL, 0.20 μmol) mixed with an CH_3CN solution of TBAB (0.50 mM, 4.0 mL, 2.0 μmol) at room temperature, and a single colorless crystal with dimensions 0.11 × 0.07 × 0.04 mm^3 was selected for intensity measurements. The unit cell was monoclinic with the space group $P2_1/n$. Lattice constants with Z = 2, ρ_{calcd} = 1.165 g cm^{-3}, $\mu(Mo_{K\alpha})$ = 0.070 mm^{-1}, $F(000)$ = 3,096, $2\theta_{max}$ = 54.94° were a = 23.940(8) Å, b = 12.658(4) Å, c = 27.816(10) Å, and V = 8,262(5) $Å^3$. A total of 52,997 reflections was collected, of which 14,120 reflections were independent (R_{int} = 0.0913). The structure was refined to final R_1 = 0.1685 for 10,034 data [$I>2\delta(I)$] with 1,159 parameters and wR_2 = 0.3334 for all data, *GOF* = 1.263, and residual electron density max/min = 0.578/–0.320 e $Å^{-3}$. The ORTEP drawing is shown in Fig. S2, and crystal data and structure refinement are listed in Table S1.

Data collection and processing were conducted using the Rigaku CrystalClear software package.[S3] The structure was solved by direct methods using SHELXS-97[S4] and refined by full-matrix least squares methods on F^2 with SHELXL-97 program[S5] using Yadokari-XG 2009.[S6] All non-hydrogen atoms were refined anisotropically. All hydrogen atoms were calculated geometrically and refined using the riding model. Crystallographic data have been deposited at the CCDC (12 Union Road, Cambridge CB2 1EZ, UK) and copies can be obtained on request, free of charge, by quoting the publication citation and the deposition number 1914679. One Level-A alert is suggested for the X-ray data by PLATON/CIF check program because the acetonitrile molecule and the pyrene unit are probably disordered. We have attempted to resolve this problem by assigning alternative positions with partial occupancies, but it did not give a better refined structure.

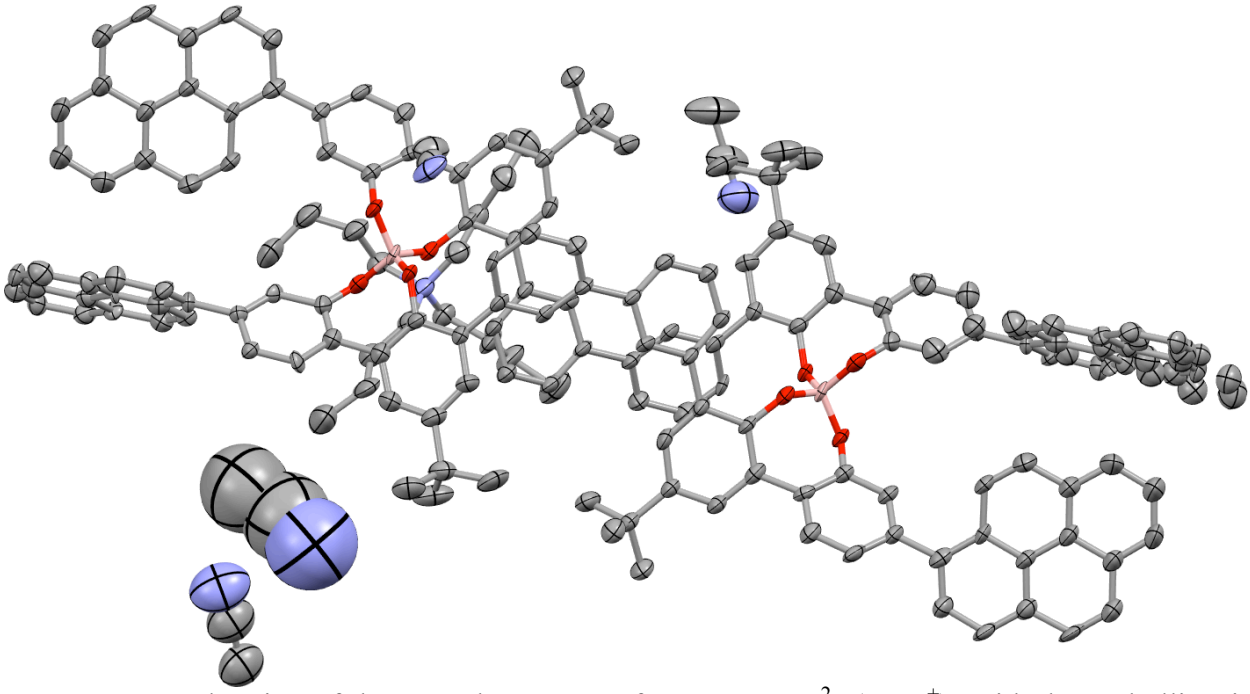

Fig. S2 ORTEP drawing of the crystal structure of *meso*-$\mathbf{DH3_{BB}}^{2-}\cdot(TBA^{+})_2$ with thermal ellipsoids at 50% probability.

Table S1 Crystal data and structure refinement for *meso*-$\mathbf{DH3_{BB}}^{2-}\cdot(TBA^{+})_2$

Empirical formula	$C_{200}H_{204}B_2N_{10}O_8$	
Formula weight	2897.35	
Temperature	103(2) K	
Wavelength	0.71075 Å	
Crystal system	Monoclinic	
Space group	$P2_1/n$	
Unit cell dimensions	a = 23.940(8) Å	α = 90.00°.
	b = 12.658(4) Å	β = 101.429(8)°.
	c = 27.816(10) Å	γ = 90.00°.
Volume	8,262(5) Å^3	
Z	2	
Density (calculated)	1.165 Mg/m^3	
Absorption coefficient	0.070 mm^{-1}	
F(000)	3,096	
Crystal size	0.11 × 0.07 × 0.04 mm^3	
Theta range for data collection	3.01 to 25.00°.	
Index ranges	-20<=h<=28, -15<=k<=11, -33<=l<=33	
Reflections collected	52,997	
Independent reflections	14,120 [R_{int} = 0.0913]	
Completeness to theta = 25.00°	97.1%	
Absorption correction	Semi-empirical from equivalents	
Max. and min. transmission	0.9972 and 0.9923	
Refinement method	Full-matrix least-squares on F^2	
Data / restraints / parameters	14,120 / 472 / 1,159	
Goodness-of-fit on F^2	1.263	
Final R indices [I>2sigma(I)]	R_1 = 0.1685, wR_2 = 0.3102	
R indices (all data)	R_1 = 0.2130, wR_2 = 0.3334	
Largest diff. peak and hole	0.578 and -0.320 e Å^{-3}	
CCDC reference number	1914679	

4. Theoretical Studies on the Structures of the Contracted ((*P*)-*rac*-$\mathbf{DH3_{BNaB}^-}$) and Extended Helicates ((*P*)-*rac*-$\mathbf{DH3_{BB}^{2-}}$).

The molecular modeling was performed on a Windows 7 PC with the ArgusLab software.[S7] The initial structures of the contracted (*rac*-$\mathbf{DH3_{BNaB}^-}$) and extended helicates (*rac*-$\mathbf{DH3_{BB}^{2-}}$) were constructed based on the crystal structures of the contracted and extended helicates with a biphenylene linker in the middle (Fig. 1a), respectively, by modification with pyrenyl residues at both ends.[S8] The initial models were then fully optimized by the density functional theory (DFT) calculations using the B3LYP functional with the LANL2DZ (for the Na^+ ion of *rac*-$\mathbf{DH3_{BNaB}^-}$) and the 6-31G* (for H, B, C, and O atoms) basis sets in *Gaussian 16* software (Gaussian, Inc., Pittsburgh, PA).[S9] The geometries were further refined by the DFT calculations using the dispersion corrected B3LYP (B3LYP-D3)[S10] functional with the LANL2DZ (for the Na^+ ion of *rac*-$\mathbf{DH3_{BNaB}^-}$), the 6-31G* (for H, C, and O atoms), and the 6-31+G* (for B atoms) basis sets in *Gaussian 16* software. Computer resources for the DFT calculations were provided by the Information Technology Center of Nagoya University. The resultant energy-minimized structures with their total energies are depicted in Fig. S3.

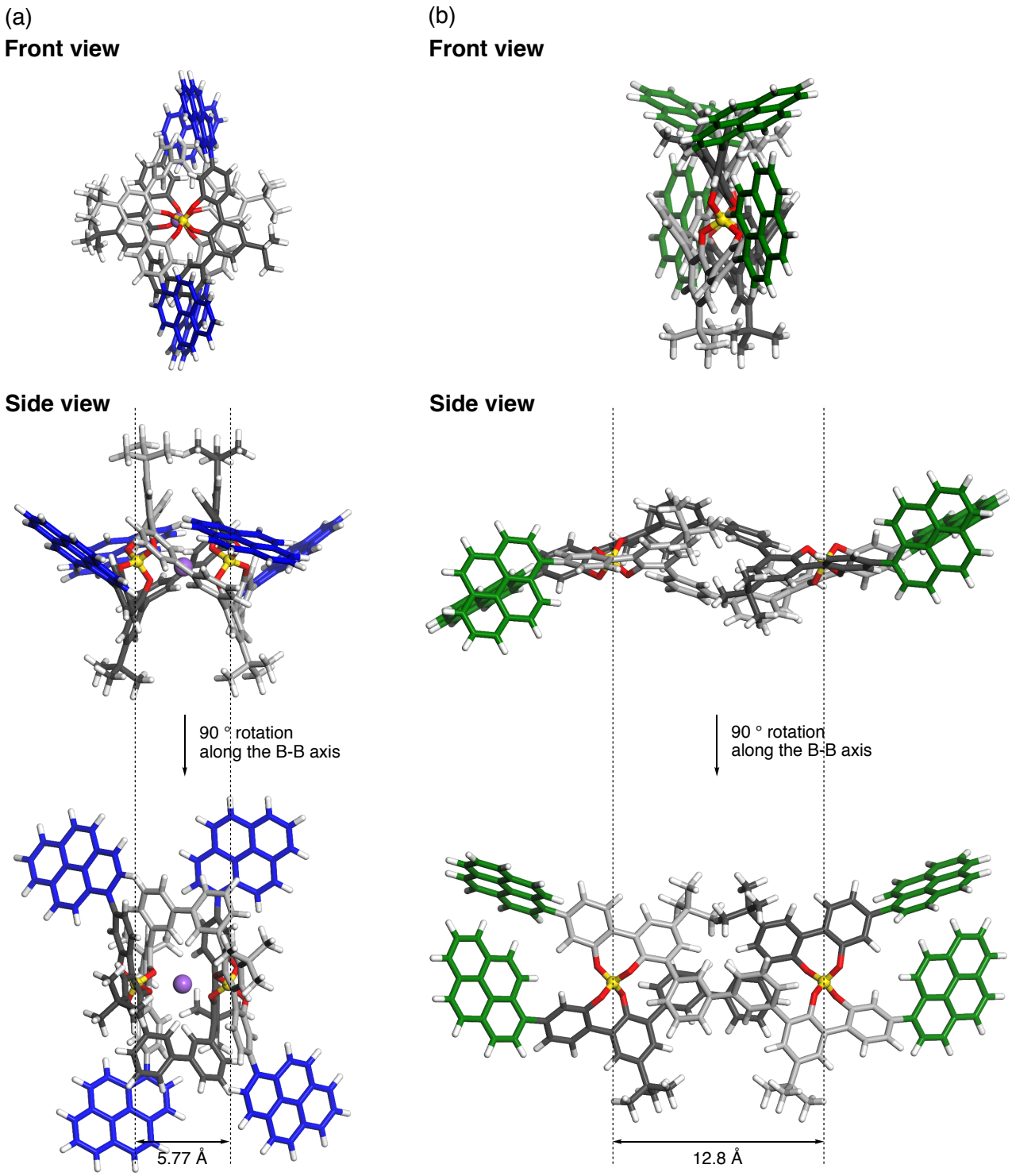

Fig. S3 The energy-minimized right-handed double-helical structures of (a) contracted (*P*)-*rac*-$\mathbf{DH3_{BNaB}}^{-}$ and (b) extended (*P*)-*rac*-$\mathbf{DH3_{BB}}^{2-}$ obtained by DFT calculations. A sodium ion (Na^{+}) is highlighted as a purple ball. DFT calculated energies are also shown in the bottom.

5. 2D NMR Spectra of *meso*-$DH3_{BB}^{2-}\cdot(Na^+)_2$ and *rac*-$DH3_{BNaB}^{-}\cdot Na^+$.

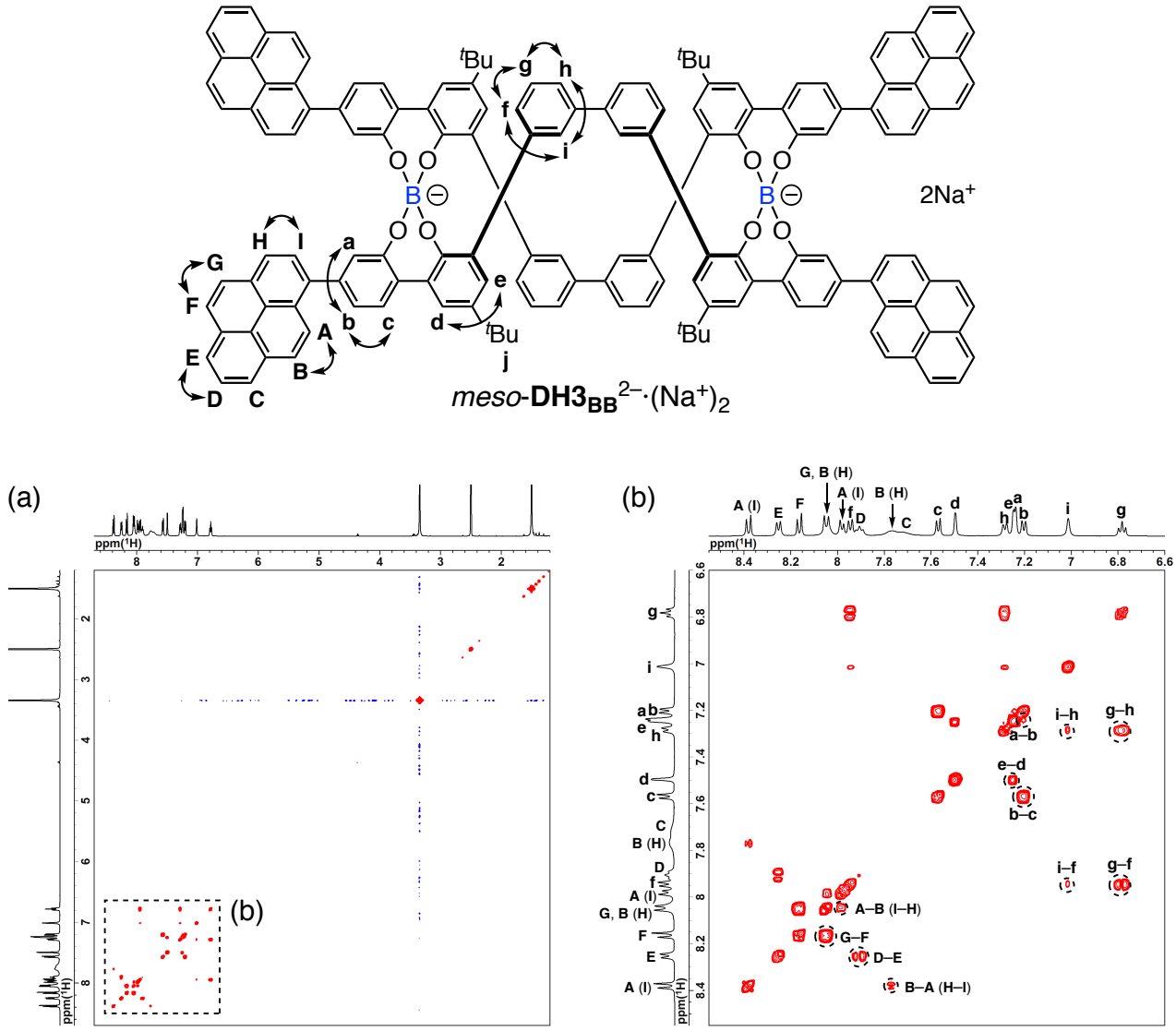

Fig. S4 (a) Full and (b) partial 500 MHz *g*COSY spectra of *meso*-$\mathbf{DH3_{BB}}^{2-}\cdot(Na^+)_2$ (DMSO-d_6, 6.6 mM, 25 °C). DMSO-d_6 was used as the solvent because of insufficient solubility of *meso*-$\mathbf{DH3_{BB}}^{2-}\cdot(Na^+)_2$ in CD_3CN for 2D NMR measurements.

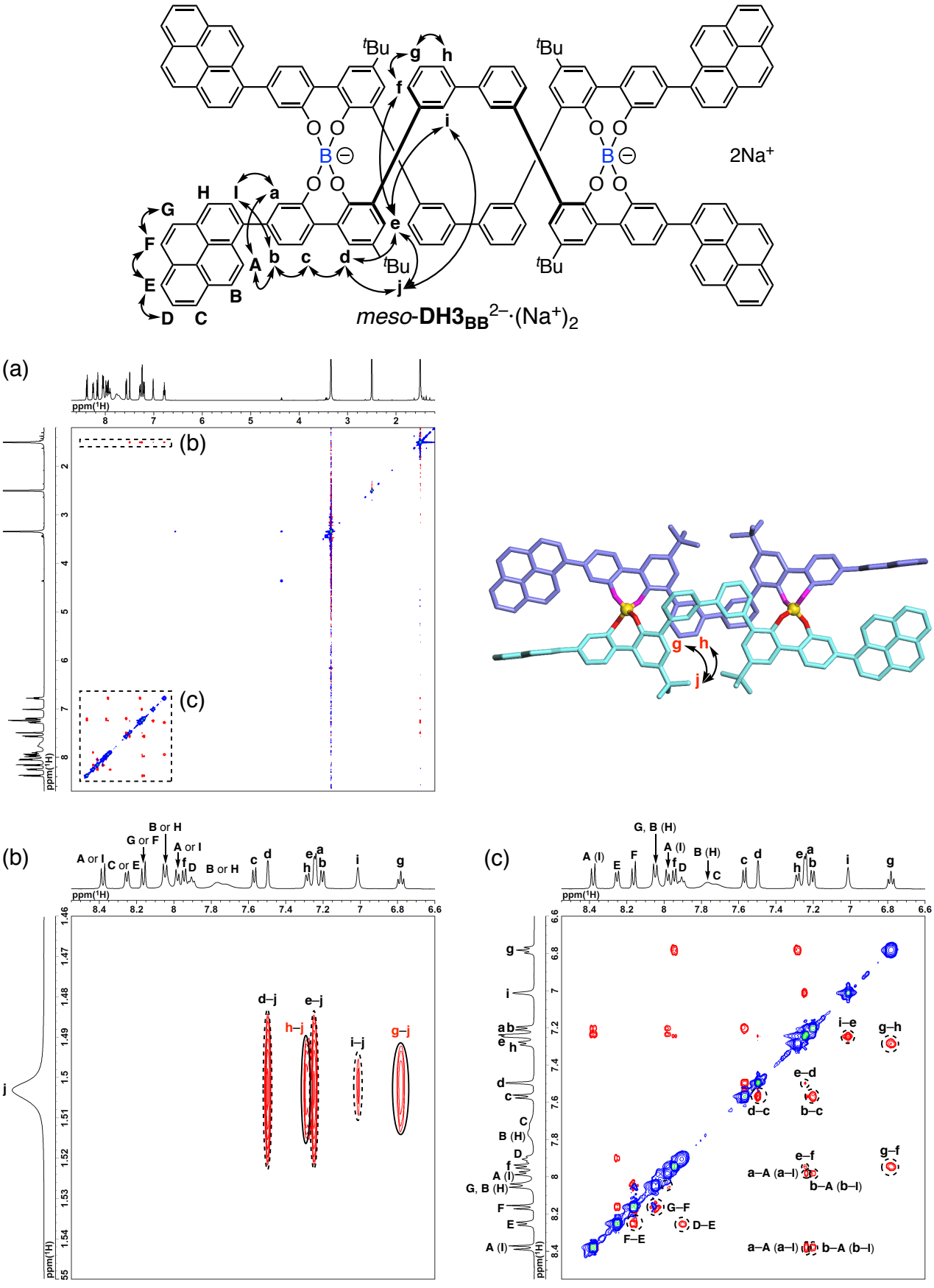

Fig. S5 (a) Full and (b) partial 500 MHz ROESY spectra of *meso*-$\mathbf{DH3_{BB}}^{2-}\cdot(Na^{+})_2$ (DMSO-d_6, 6.6 mM, 25 °C, mixing time = 200 ms).

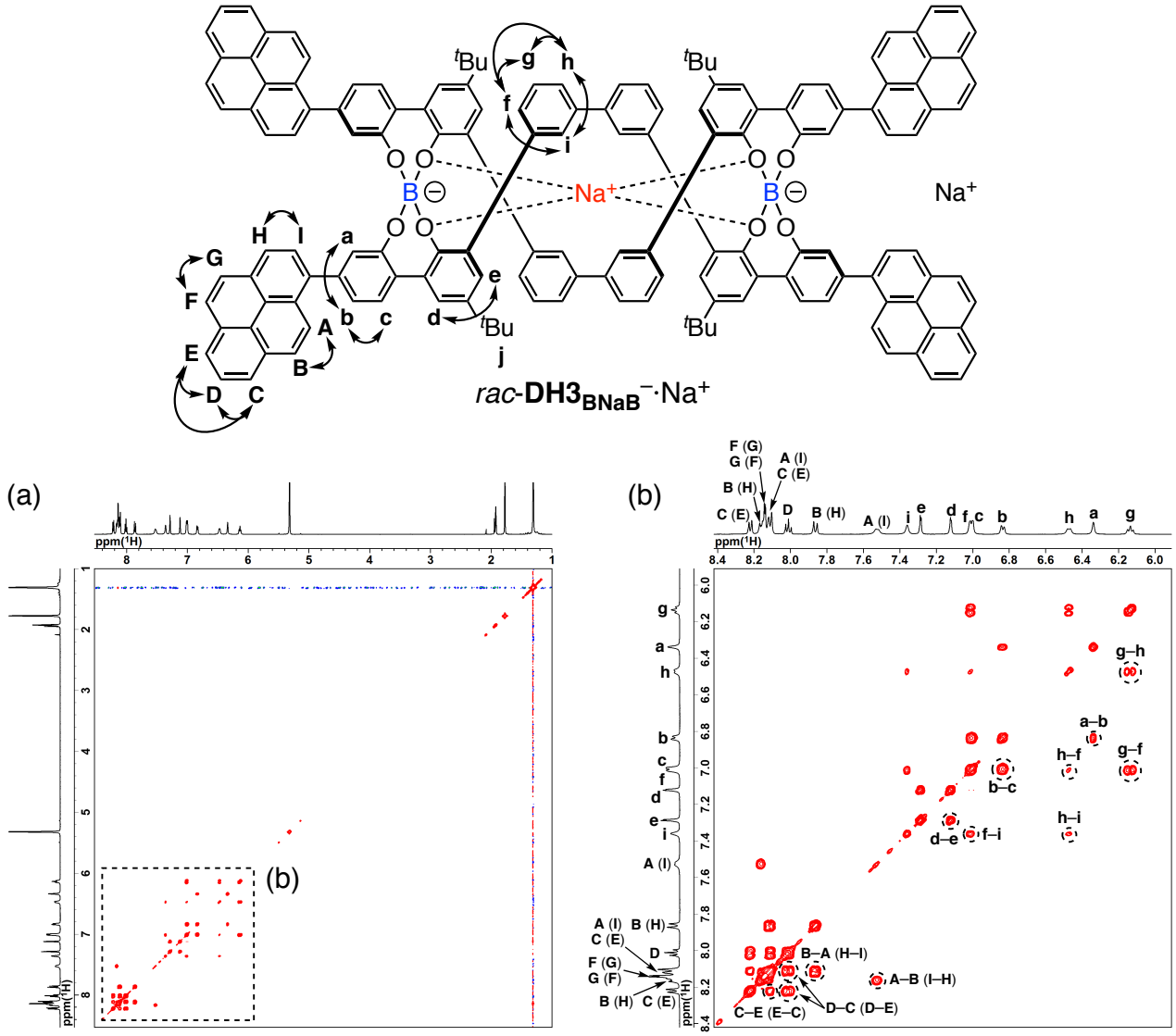

Fig. S6 (a) Full and (b) partial 500 MHz *g*COSY spectra of *rac*-**DH3$_{BNaB}$**$^{-}$·Na^{+} (CD_2Cl_2/CD_3CN = 6/1 (v/v), 2.0 mM, 25 °C).

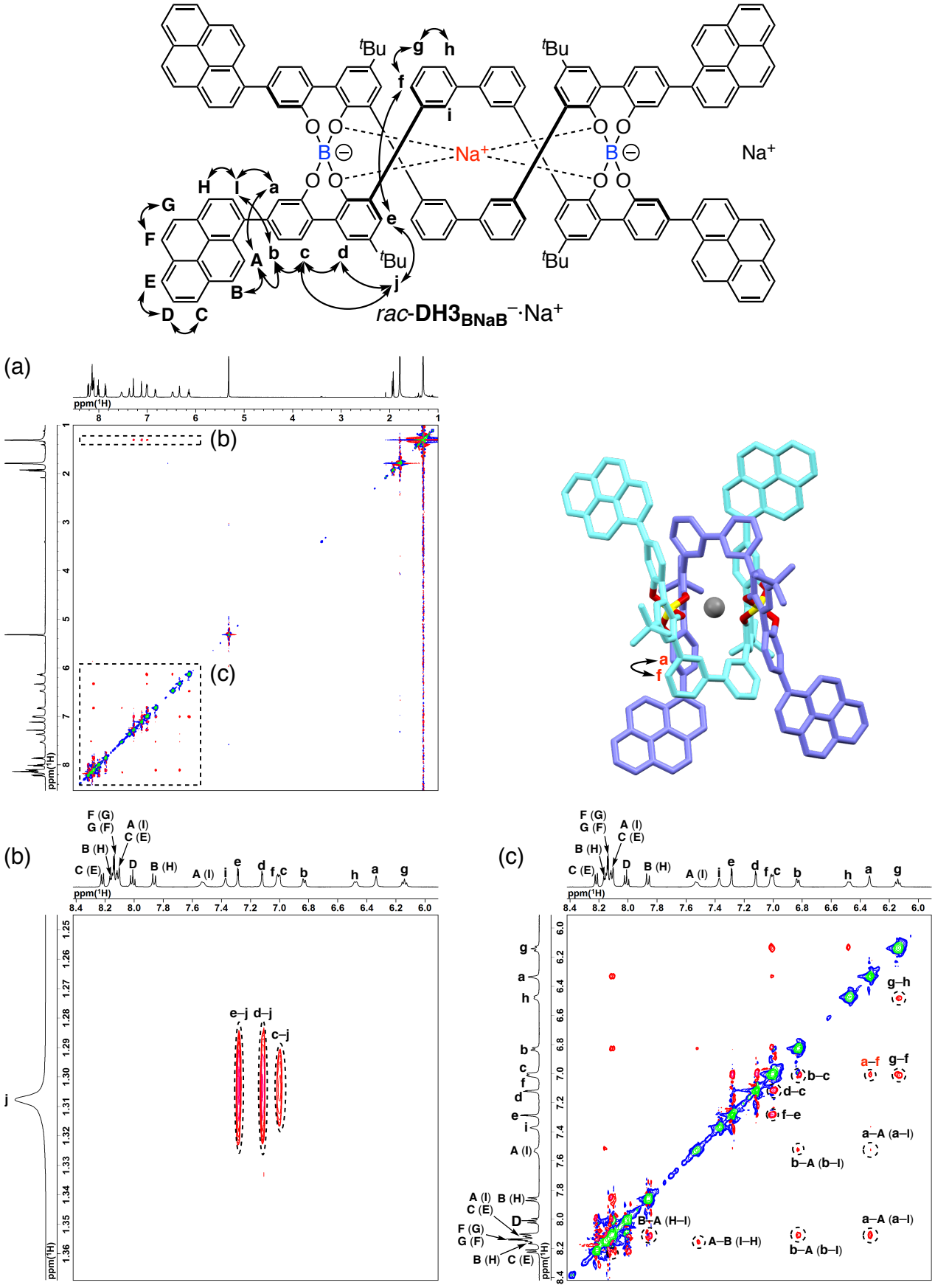

Fig. S7 (a) Full and (b) partial 500 MHz ROESY spectra of *rac*-**DH3**$_{\mathbf{BNaB}}^{-}$·Na^+ (CD_2Cl_2/CD_3CN = 6/1 (v/v), 2.0 mM, 25 °C, mixing time = 200 ms).

6. ^{1}H NMR, Absorption and Fluorescence spectra of *meso*-DH3$_{BB}^{2-}$·(Na$^+$)$_2$ in the Absence and Presence of Cryptand[2.2.1].

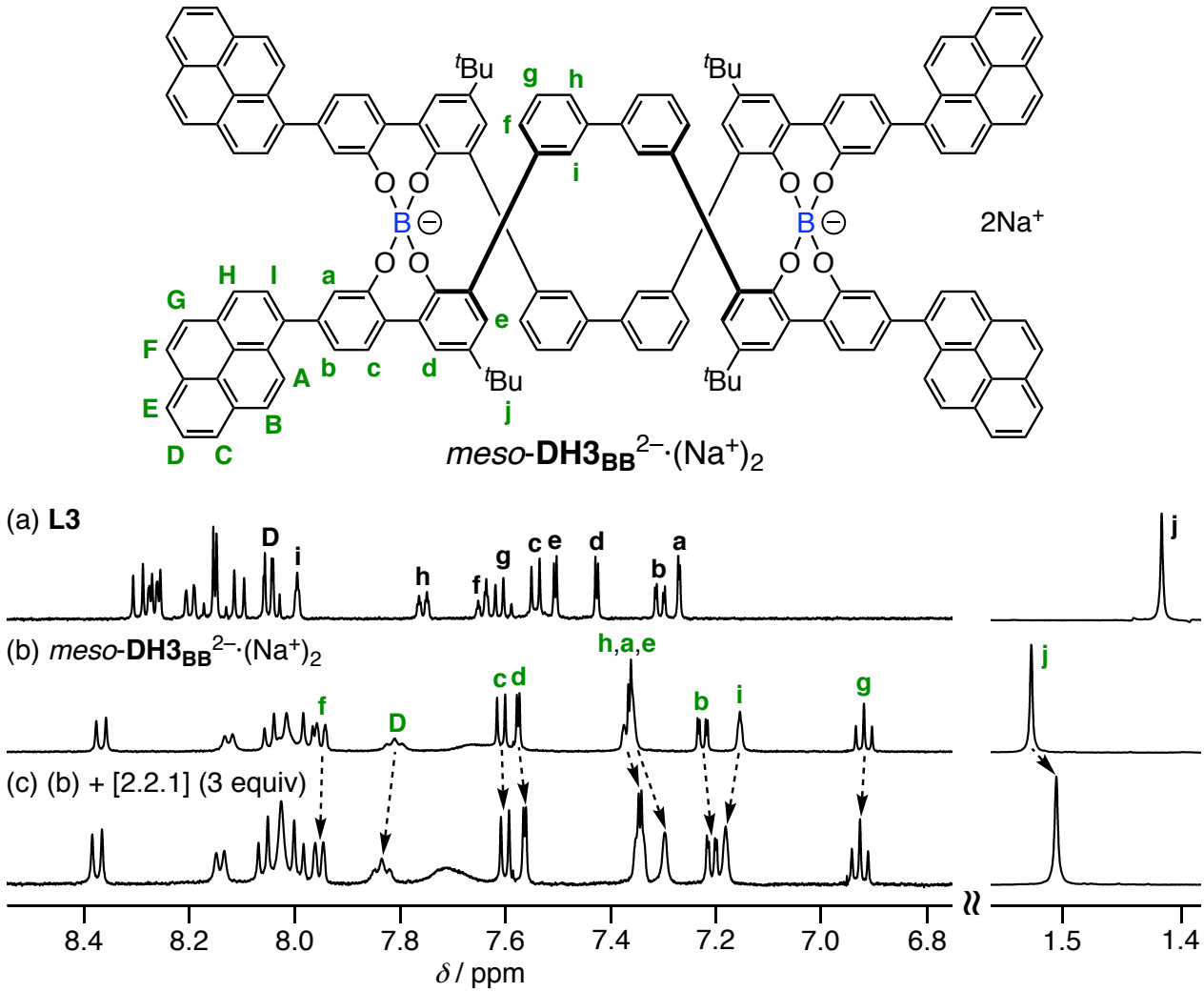

Fig. S8 Partial ^{1}H NMR spectra (500 MHz, CD_3CN, 0.50 mM, rt) of (a) **L3**, (b) *meso*-DH3$_{BB}^{2-}$·(Na$^+$)$_2$, and (c) (b) + [2.2.1] (3 equiv).

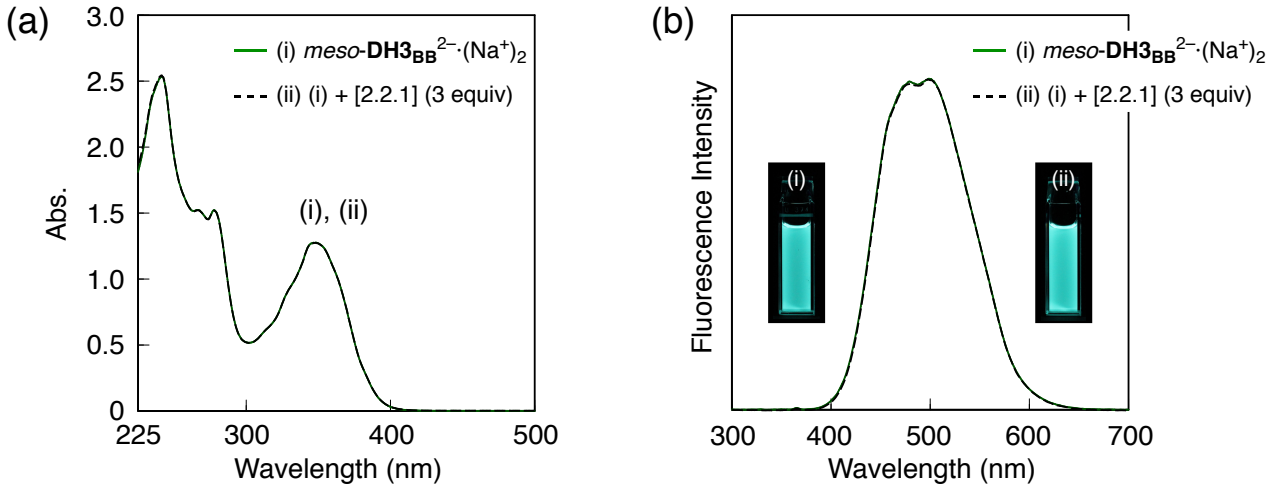

Fig. S9 (a) Absorption and (b) fluorescence spectra (CH_3CN, 10 μM, rt) of (i) *meso*-$\mathbf{DH3_{BB}}^{2-}$·$(Na^+)_2$ and (ii) (i) + [2.2.1] (3 equiv). Excited wavelength: 365 nm. Photographs of *meso*-$\mathbf{DH3_{BB}}^{2-}$·$(Na^+)_2$ (10 μM) before and after the addition of [2.2.1] (3 equiv) in CH_3CN under irradiation at 365 nm are also shown in (b).

7. Optical Resolution of (±)-*rac*-DH3$_{BNaB}^{-}$·Na^{+} by Chiral HPLC. The optical resolution of the boron helicate (±)- *rac*-**DH3**$_{BNaB}^{-}$·Na^{+} was performed by chiral HPLC using a chiral column (CHIRALPAK IB, Daicel, Co., Ltd.) with *n*-hexane/$CHCl_3$ = 6/4 (v/v) containing *n*-tetrabutylammonium bromide (TBAB) (0.5 mg/mL) as the eluent (Fig. S10).

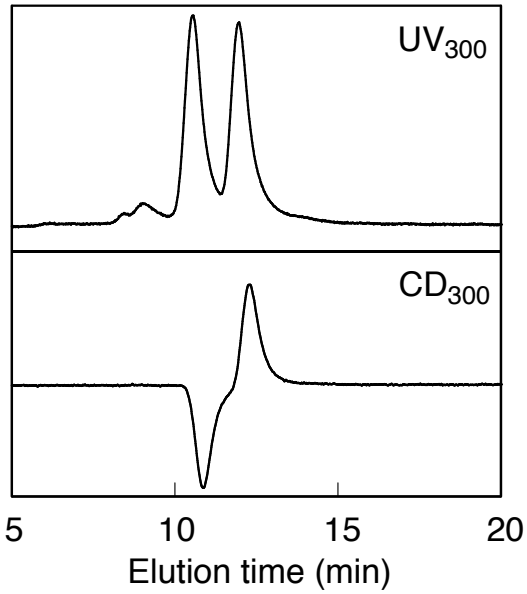

Fig. S10 UV (upper) and CD (bottom) (300 nm) detected HPLC chromatograms of *rac*-**DH3**$_{BNaB}^{-}$·Na^{+}. HPLC conditions: column, CHIRALPAK IB (Daicel, 0.46 (i.d.) × 25 cm); eluent, *n*-hexane/$CHCl_3$ = 6/4 (v/v) containing TBA^{+}·Br^{-} (0.5 mg/mL); flow rate, 1.0 mL/min; column temperature, 25 °C.

8. Determination of the Association Constants of *rac*-$\mathbf{DH3_{BB}}^{2-}\cdot(Na^+\subset[2.2.1])_2$ with a Na^+ Ion in Different Solvents.

The association constants (K_a) of *rac*-$\mathbf{DH3_{BB}}^{2-}\cdot(Na^+\subset[2.2.1])_2$ with Na^+ in CD_3CN and CH_2Cl_2/CH_3CN = 6/1 (v/v), respectively, were directly estimated by ^1H NMR and fluorescence titrations (Fig. S11a and S12a). The chemical shift changes ($|\Delta\delta|$) of the peak for the *t*-Bu proton and fluorescence intensity changes (ΔFl) at 442 nm of *rac*-$\mathbf{DH3_{BB}}^{2-}\cdot(Na^+\subset[2.2.1])_2$ were plotted versus the concentration of $NaN(SO_2CF_3)_2$ and the K_a values were calculated based on the curve-fitting method (1:1 binding model) using the following equations (Fig. S11b and S12b).

$$|\Delta\delta| = \frac{|\Delta\delta_{max}|}{2K_a[\mathrm{NaN(SO_2CF_3)_2}]}\Big[1+K_a[\mathrm{NaN(SO_2CF_3)_2}]+K_a[\textit{rac}\text{-}\mathbf{DH3_{BB}}^{2-}\cdot(Na^+\subset[2.2.1])_2] - \sqrt{\left(1+K_a[\mathrm{NaN(SO_2CF_3)_2}]+K_a[\textit{rac}\text{-}\mathbf{DH3_{BB}}^{2-}\cdot(Na^+\subset[2.2.1])_2]\right)^2 - 4K_a{}^2[\mathrm{NaN(SO_2CF_3)_2}][\textit{rac}\text{-}\mathbf{DH3_{BB}}^{2-}\cdot(Na^+\subset[2.2.1])_2]}\Big]$$

$$\Delta Fl = \frac{\Delta Fl_{max}}{2K_a[\mathrm{NaN(SO_2CF_3)_2}]}\Big[1+K_a[\mathrm{NaN(SO_2CF_3)_2}]+K_a[\textit{rac}\text{-}\mathbf{DH3_{BB}}^{2-}\cdot(Na^+\subset[2.2.1])_2] - \sqrt{\left(1+K_a[\mathrm{NaN(SO_2CF_3)_2}]+K_a[\textit{rac}\text{-}\mathbf{DH3_{BB}}^{2-}\cdot(Na^+\subset[2.2.1])_2]\right)^2 - 4K_a{}^2[\mathrm{NaN(SO_2CF_3)_2}][\textit{rac}\text{-}\mathbf{DH3_{BB}}^{2-}\cdot(Na^+\subset[2.2.1])_2]}\Big]$$

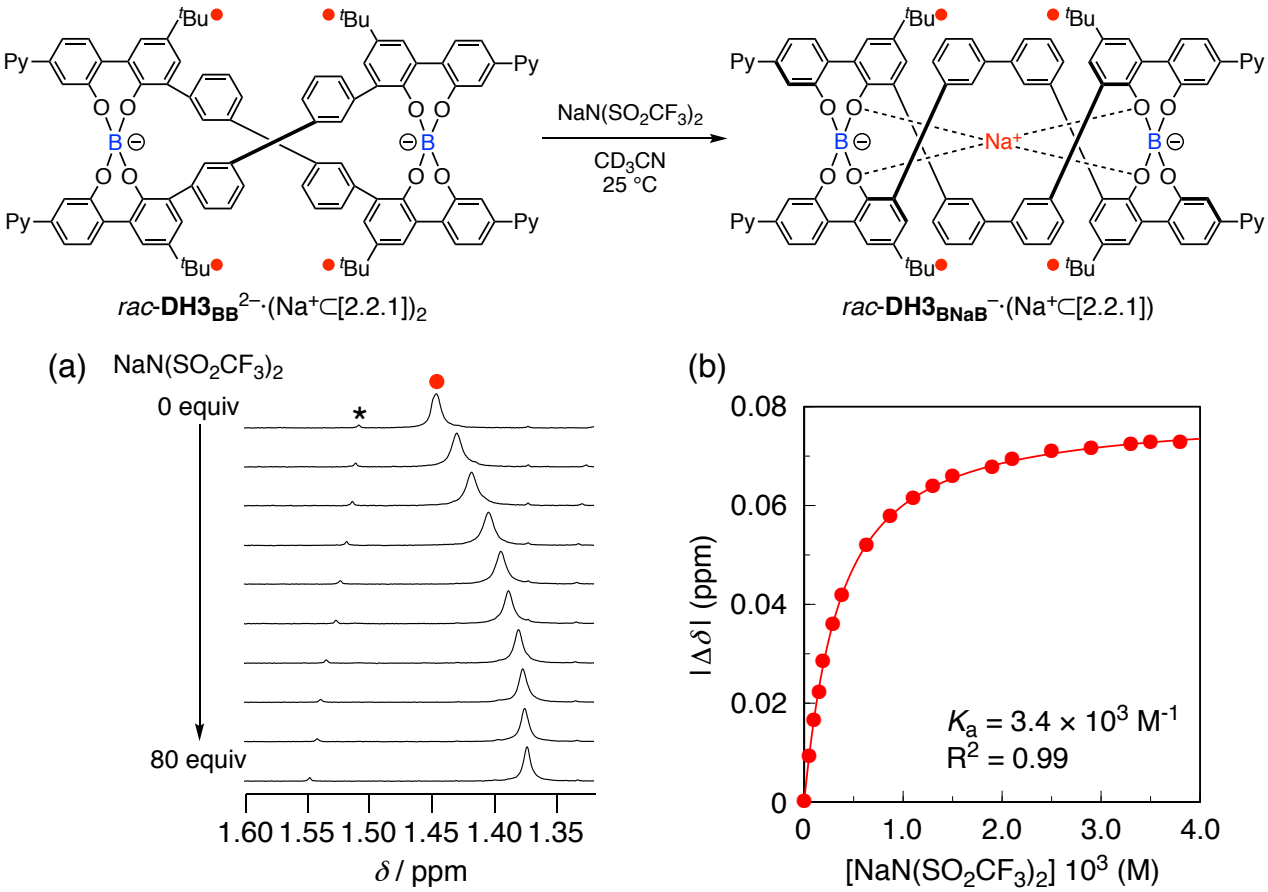

Fig. S11 (a) Partial ^{1}H NMR spectra (500 MHz, CD_3CN, 0.10 mM, 25 °C) of *rac*-**DH3$_{BB}$**$^{2-}$·(Na^+⊂[2.2.1])$_2$ containing *meso*-**DH3$_{BB}$**$^{2-}$·(Na^+⊂[2.2.1])$_2$ (ca. 2–3 mol%) in the presence of $NaN(SO_2CF_3)_2$ (0–80 equiv). * denotes the ^{t}Bu proton from *meso*-**DH3$_{BB}$**$^{2-}$·(Na^+⊂[2.2.1])$_2$. (b) Plots of the ^{t}Bu chemical shift changes ($|\Delta\delta|$) versus the concentration of $NaN(SO_2CF_3)_2$ in CD_3CN. The curve in the plots was obtained by the curve-fitting method (1:1 binding model), giving the association constant (K_a) of *rac*-**DH3$_{BB}$**$^{2-}$·(Na^+⊂[2.2.1])$_2$ with Na^+ in CD_3CN to be 3.4×10^3 M^{-1}.

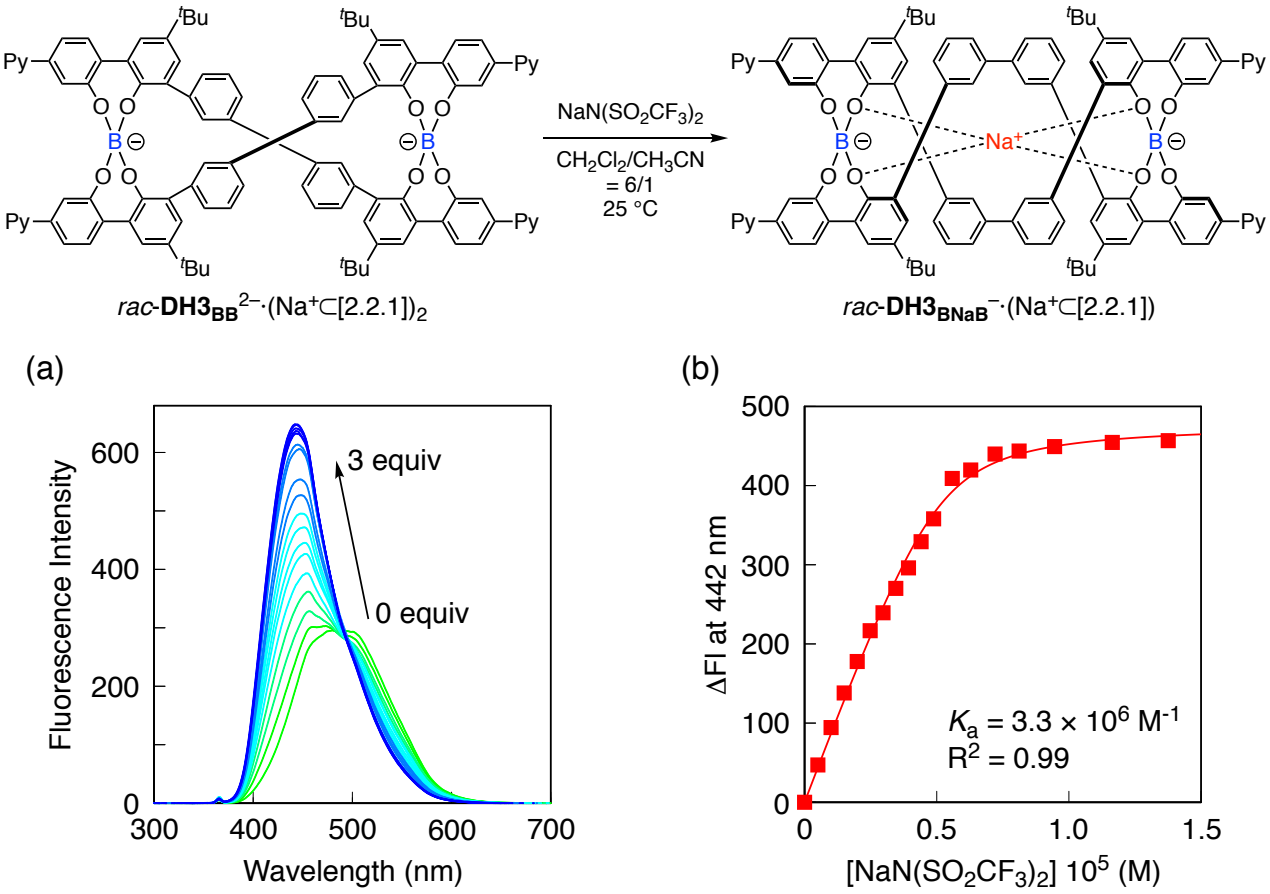

Fig. S12 (a) Fluorescence titrations of *rac*-$\mathbf{DH3_{BB}}^{2-}$·(Na^+⊂[2.2.1])$_2$ (4.9 μM) with $NaN(SO_2CF_3)_2$ in CH_2Cl_2/CH_3CN = 6/1 (v/v) at 25°C. Excited wavelength: 365 nm. (b) Plots of fluorescence intensity changes (ΔFl) at 442 nm for *rac*-$\mathbf{DH3_{BB}}^{2-}$·(Na^+⊂[2.2.1])$_2$ versus the concentration of [$NaN(SO_2CF_3)_2$]. The curve in the plots was obtained by the curve-fitting method (1:1 binding model), giving the association constant (K_a) of *rac*-$\mathbf{DH3_{BB}}^{2-}$·(Na^+⊂[2.2.1])$_2$ with Na^+ in CH_2Cl_2/CH_3CN = 6/1 (v/v) to be 3.3×10^6 M^{-1}.

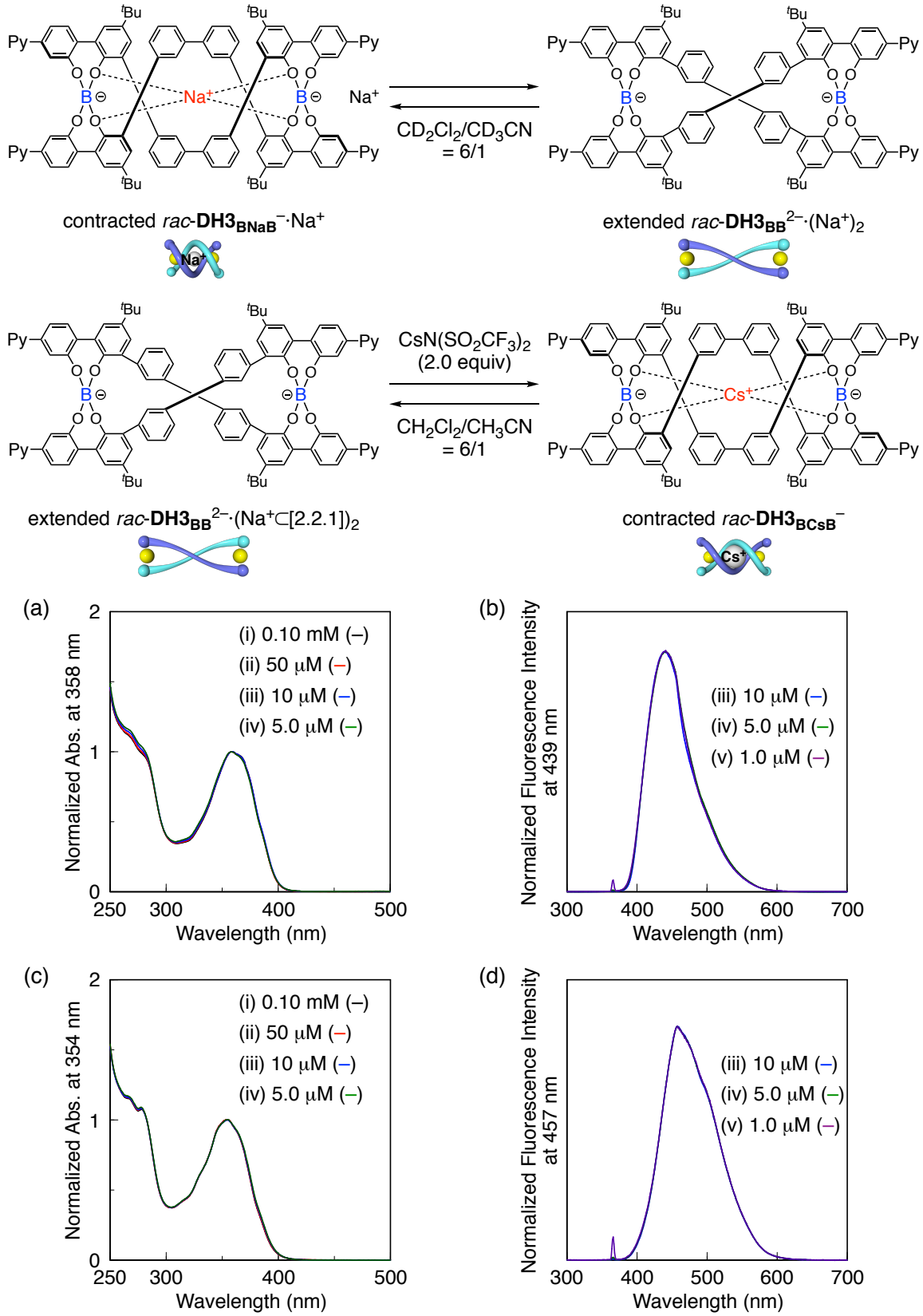

Fig. S13 (a–d) Concentration-dependent (a,c) absorption and (b,d) fluorescence spectral changes of *rac*-**DH3**$_{\mathbf{BNaB}}^{-}$·Na^+ and *rac*-**DH3**$_{\mathbf{BB}}^{2-}$·(Na^+⊂[2.2.1])$_2$ in the presence of $CsN(SO_2CF_3)_2$ (2.0 equiv) ((i) 0.10 mM, (ii) 50, (iii) 10, (iv) 5.0 and (v) 1.0 μM) in CD_2Cl_2/CD_3CN = CH_2Cl_2/CH_3CN = 6/1 (v/v) at (a,c) 25 °C and (b,d) rt. Excited wavelength: 365 nm. The absorption and fluorescence intensities were normalized at (a) 358 and (c) 354, and (b) 439 and (d) 457 nm, respectively.

9. Supporting References.

S1 A. Inoue, K. Kitagawa, H. Shinokubo and K. Oshima, *Tetrahedron*, 2000, **56**, 9601–9605.

S2 K. Miwa, K. Shimizu, H. Min, Y. Furusho and E. Yashima, *Tetrahedron*, 2012, **68**, 4470–4478.

S3 CrystalClear, Version 1.36; Molecular Structure Corporation: The Woodlands, TX, 2000 and Rigaku Corporation: Tokyo, Japan.

S4 G. M. Sheldrick, SHELXS-97: Program for the Solution of Crystal Structures; University of Göttingen, Göttingen, Germany, 1997.

S5 (a) G. M. Sheldrick, SHELXL-97: Program for the Refinement of Crystal Structures; University of Göttingen, Göttingen, Germany, 1997. (b) G. M. Sheldrick, *Acta Crystallogr.*, 2008, **A64**, 112–122.

S6 (a) K. Wakita, *Yadokari-XG,* Program for Crystal Structure Analysis; 2000. (b) C. Kabuto, S. Akine and E. Kwon, *J. Cryst. Soc. Jpn.*, 2009, **51**, 218–224.

S7 M. Thompson, ArgusLab, Planaria Software LLC, Seattle, WA (1996).

S8 K. Miwa, Y. Furusho and E. Yashima, *Nat. Chem.*, 2010, **2**, 444–449.

S9 Gaussian 16, Revision A.03, M. J. Frisch, G. W. Trucks, H. B. Schlegel, G. E. Scuseria, M. A. Robb, J. R. Cheeseman, G. Scalmani, V. Barone, G. A. Petersson, H. Nakatsuji, X. Li, M. Caricato, A. V. Marenich, J. Bloino, B. G. Janesko, R. Gomperts, B. Mennucci, H. P. Hratchian, J. V. Ortiz, A. F. Izmaylov, J. L. Sonnenberg, D. Williams-Young, F. Ding, F. Lipparini, F. Egidi, J. Goings, B. Peng, A. Petrone, T. Henderson, D. Ranasinghe, V. G. Zakrzewski, J. Gao, N. Rega, G. Zheng, W. Liang, M. Hada, M. Ehara, K. Toyota, R. Fukuda, J. Hasegawa, M. Ishida, T. Nakajima, Y. Honda, O. Kitao, H. Nakai, T. Vreven, K. Throssell, J. A. Montgomery, Jr., J. E. Peralta, F. Ogliaro, M. J. Bearpark, J. J. Heyd, E. N. Brothers, K. N. Kudin, V. N. Staroverov, T. A. Keith, R. Kobayashi, J. Normand, K. Raghavachari, A. P. Rendell, J. C. Burant, S. S. Iyengar, J. Tomasi, M. Cossi, J. M. Millam, M. Klene, C. Adamo, R. Cammi, J. W. Ochterski, R. L. Martin, K. Morokuma, O. Farkas, J. B. Foresman and D. J. Fox, Gaussian, Inc., Wallingford CT, 2016.

S10 S. Grimme, J. Antony, S. Ehrlich and H. Krieg, *J. Chem. Phys*., 2010, **132**, 154104.

10. Spectroscopic Data

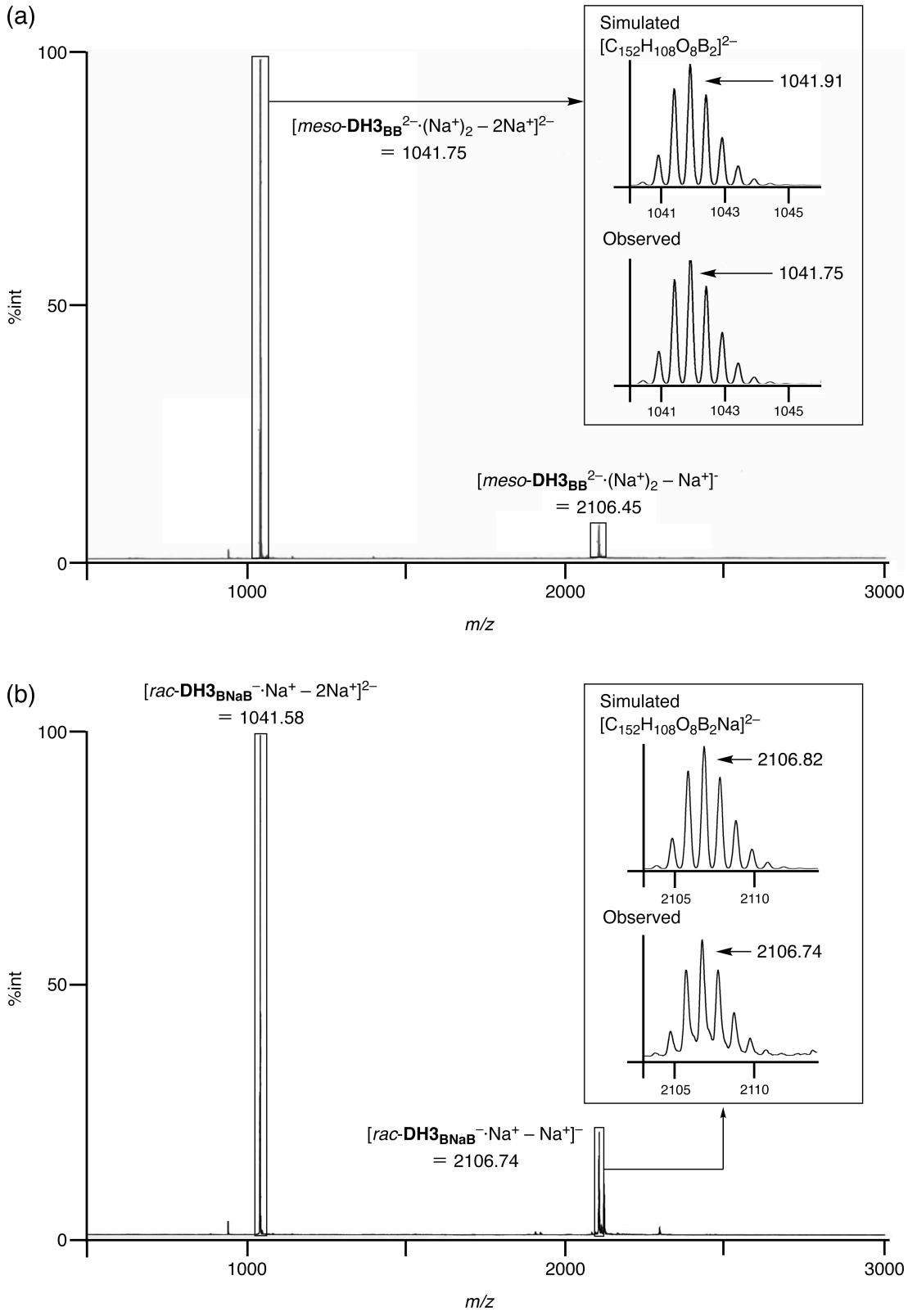

Fig. S14 Negative mode ESI mass spectra of (a) *meso*-$\mathbf{DH3_{BB}}^{2-}\cdot(Na^+)_2$ and (b) *rac*-$\mathbf{DH3_{BNaB}}^{-}\cdot Na^+$.

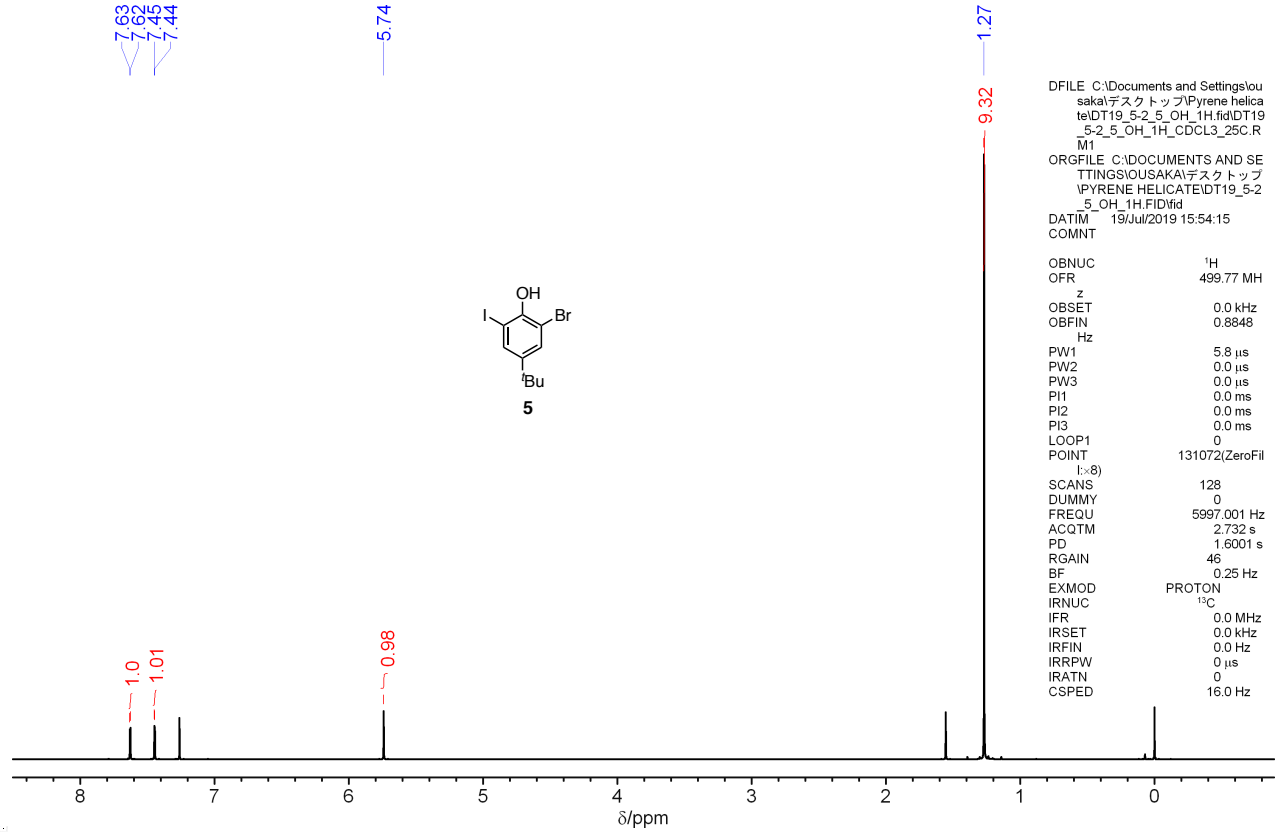

Fig. S15 ^{1}H NMR spectrum of **5** in $CDCl_3$ at 25 ºC.

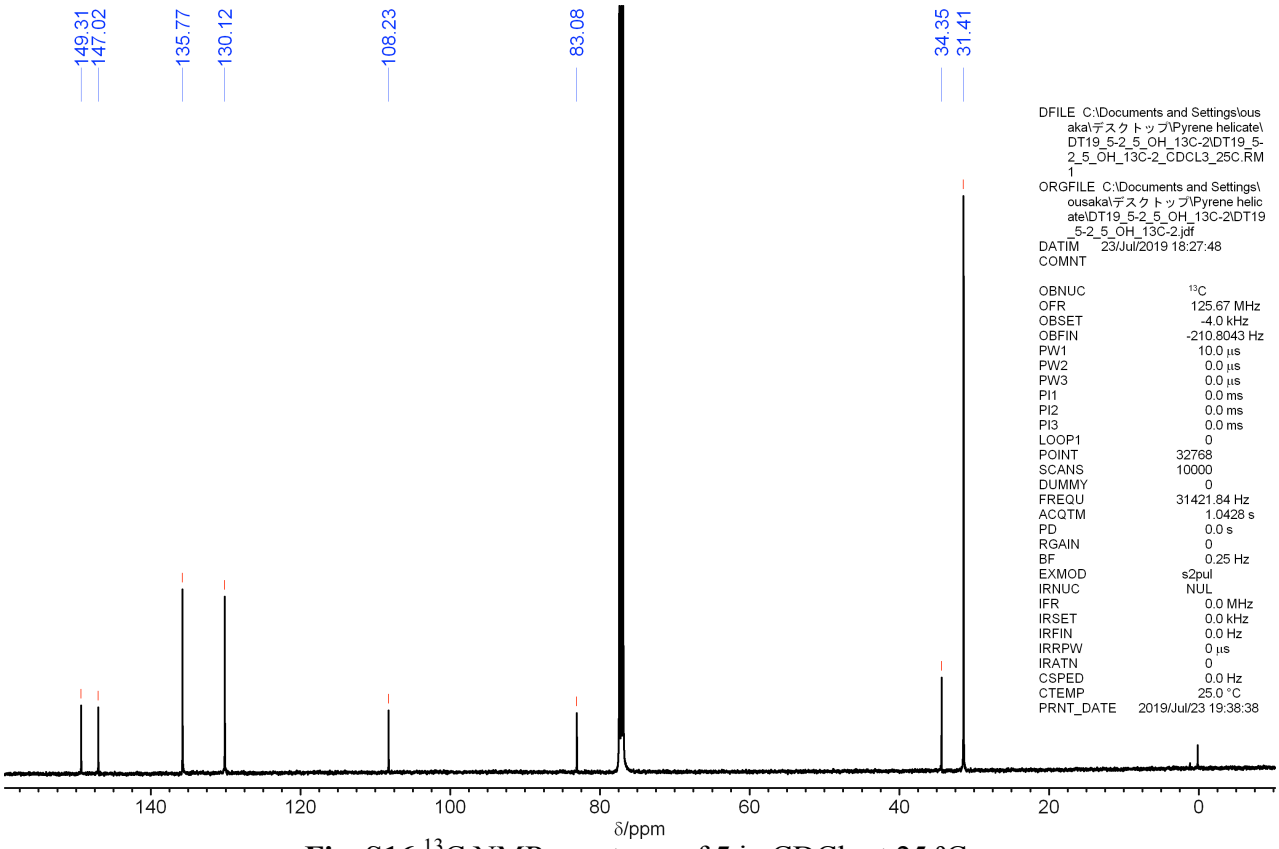

Fig. S16 ^{13}C NMR spectrum of **5** in $CDCl_3$ at 25 ºC.

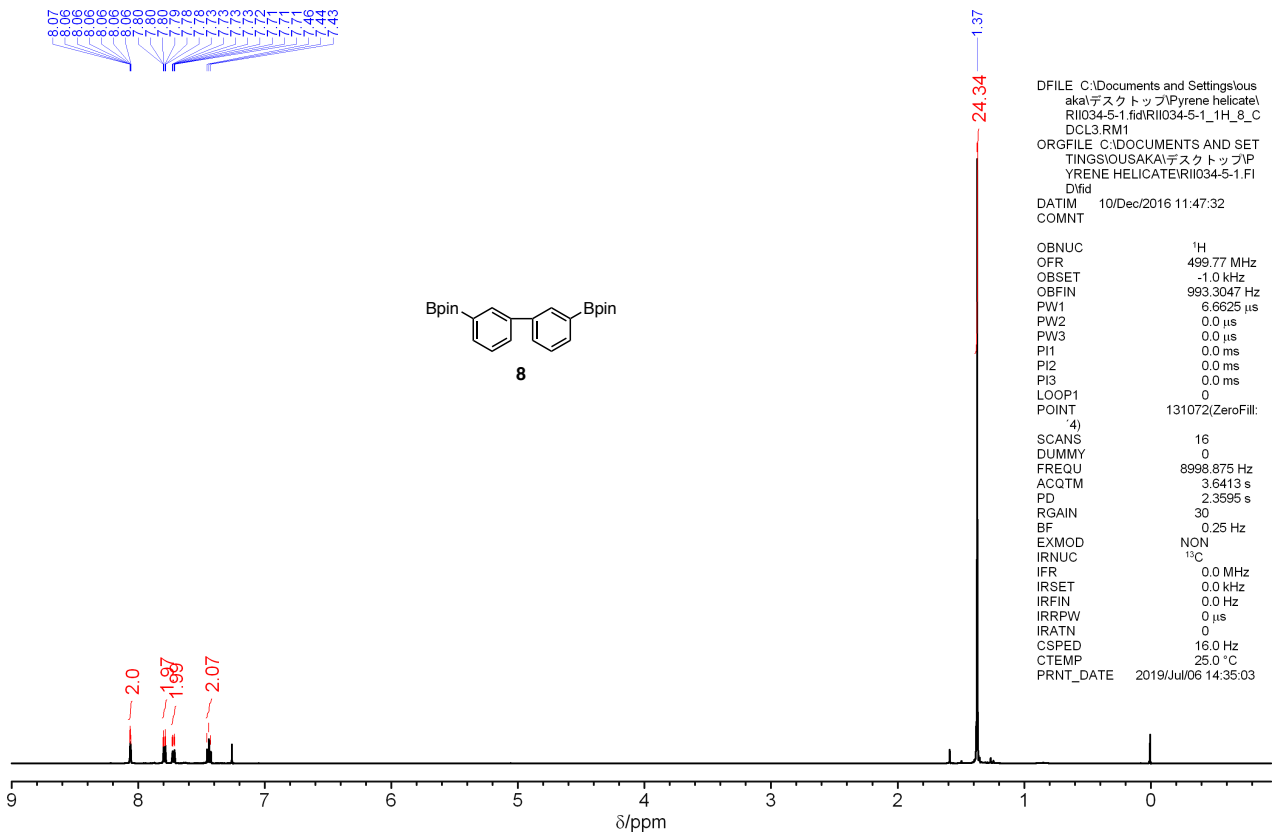

Fig. S17 ^{1}H NMR spectrum of **8** in $CDCl_3$ at 25 ºC.

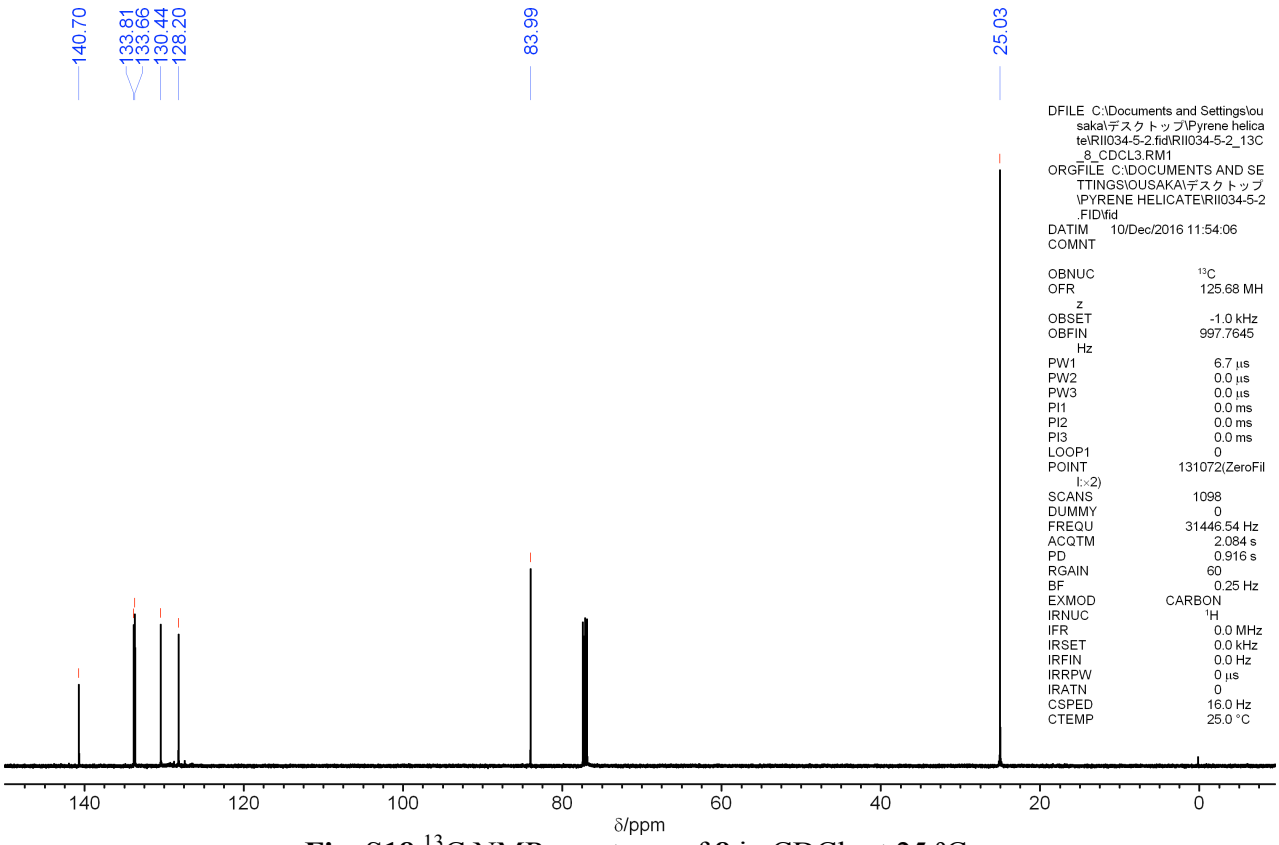

Fig. S18 ^{13}C NMR spectrum of **8** in $CDCl_3$ at 25 ºC.

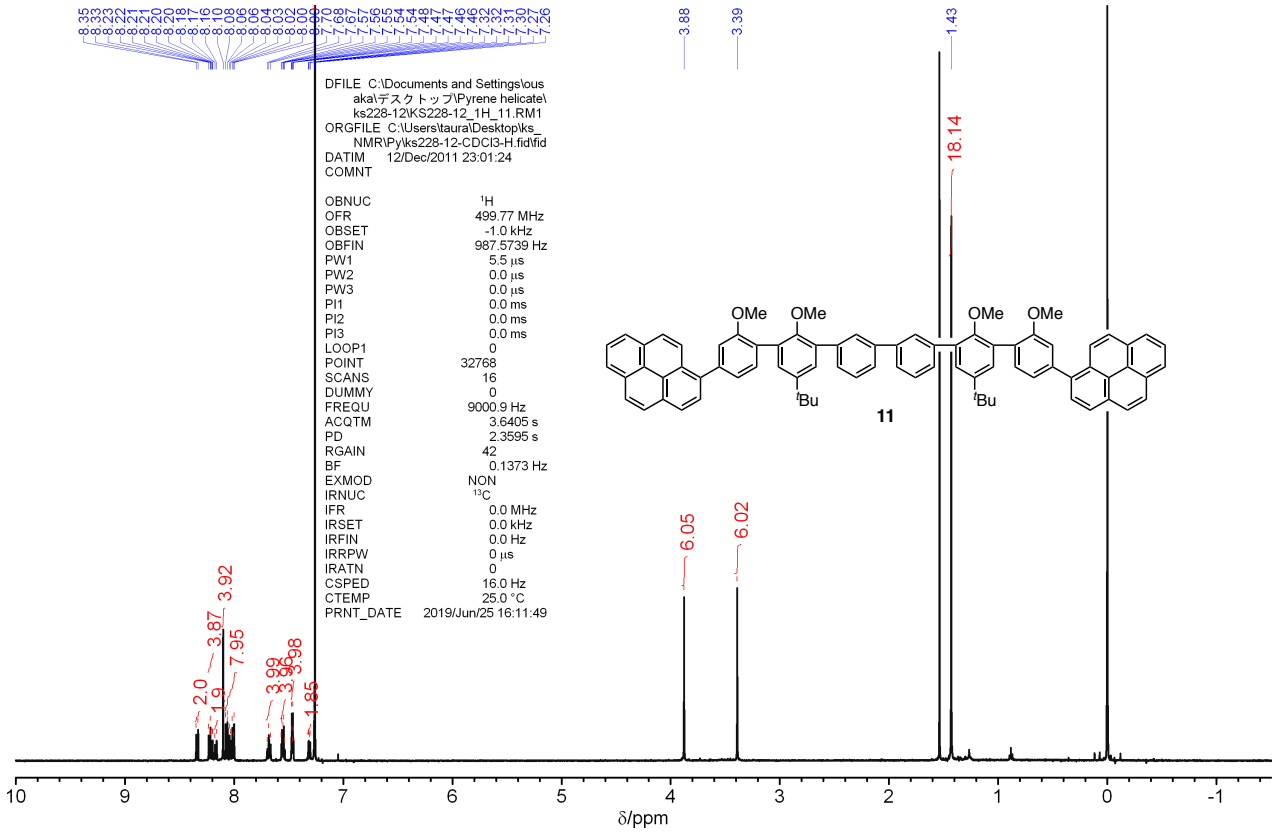

Fig. S19 ^{1}H NMR spectrum of **11** in $CDCl_3$ at 25 ºC.

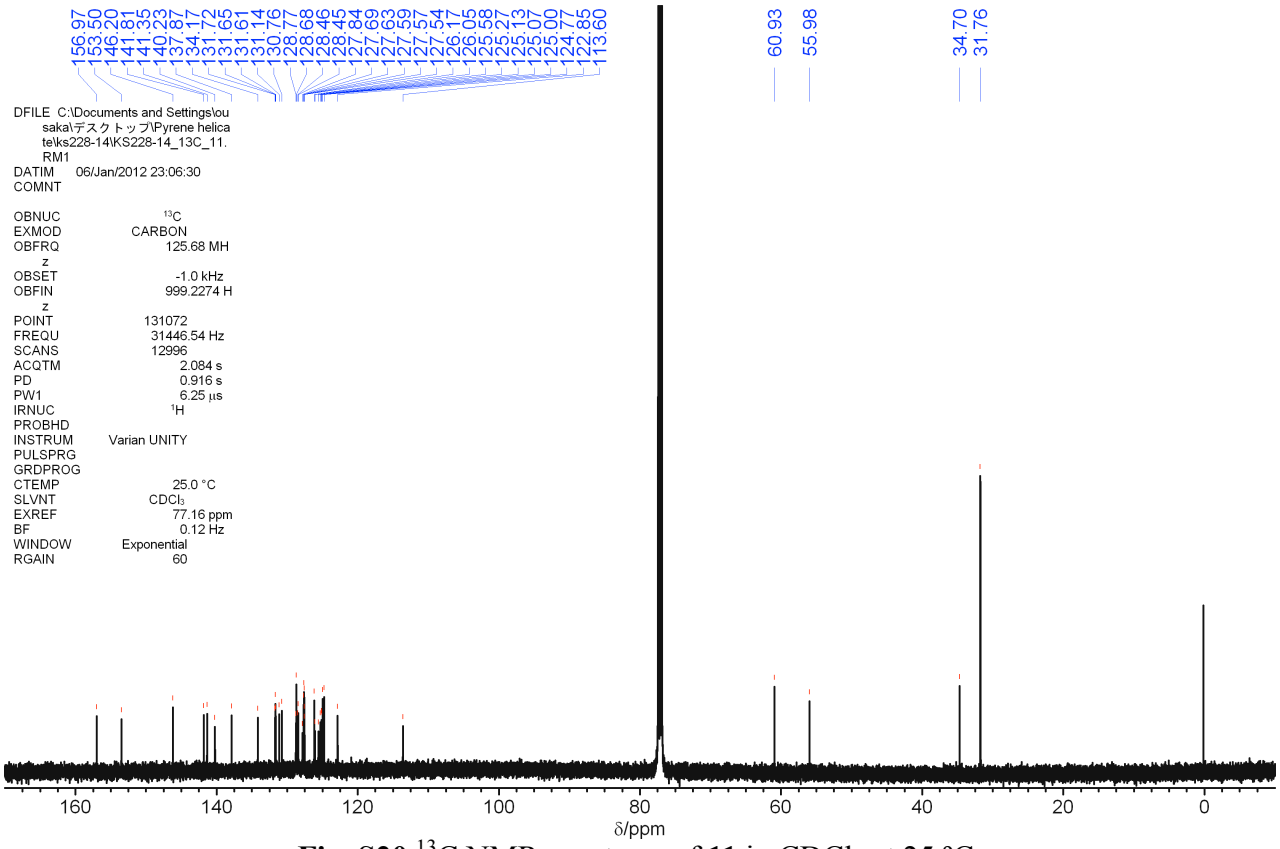

Fig. S20 ^{13}C NMR spectrum of **11** in $CDCl_3$ at 25 ºC.

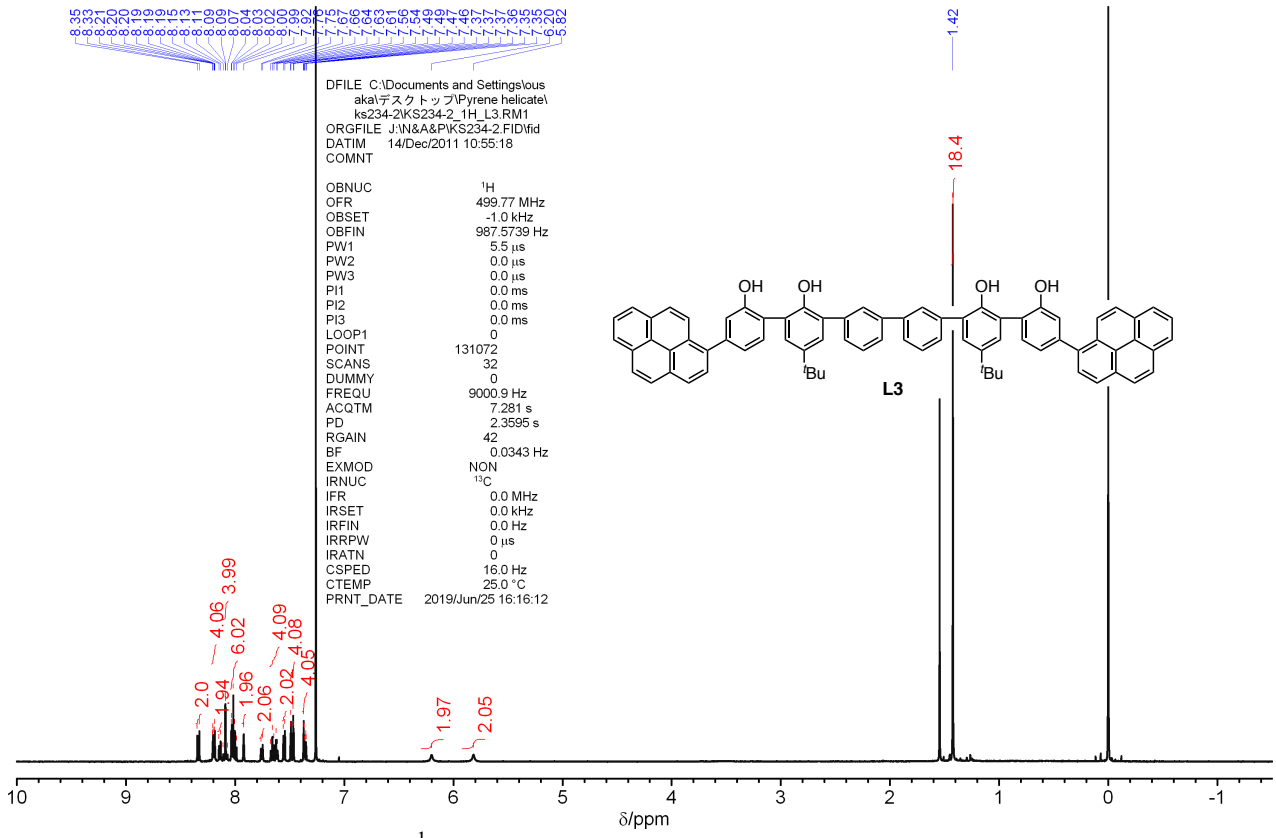

Fig. S21 ^{1}H NMR spectrum of **L3** in $CDCl_3$ at 25 ºC.

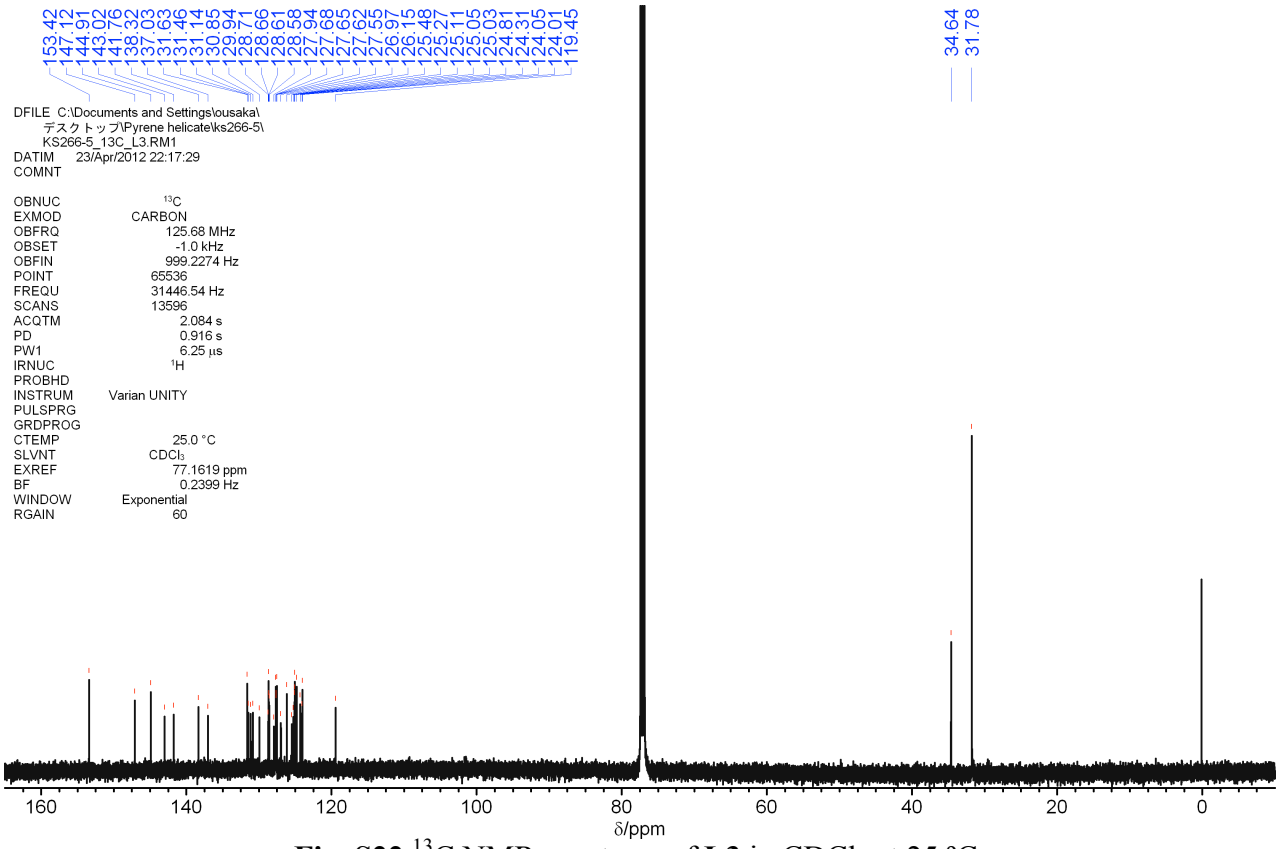

Fig. S22 ^{13}C NMR spectrum of **L3** in $CDCl_3$ at 25 ºC.

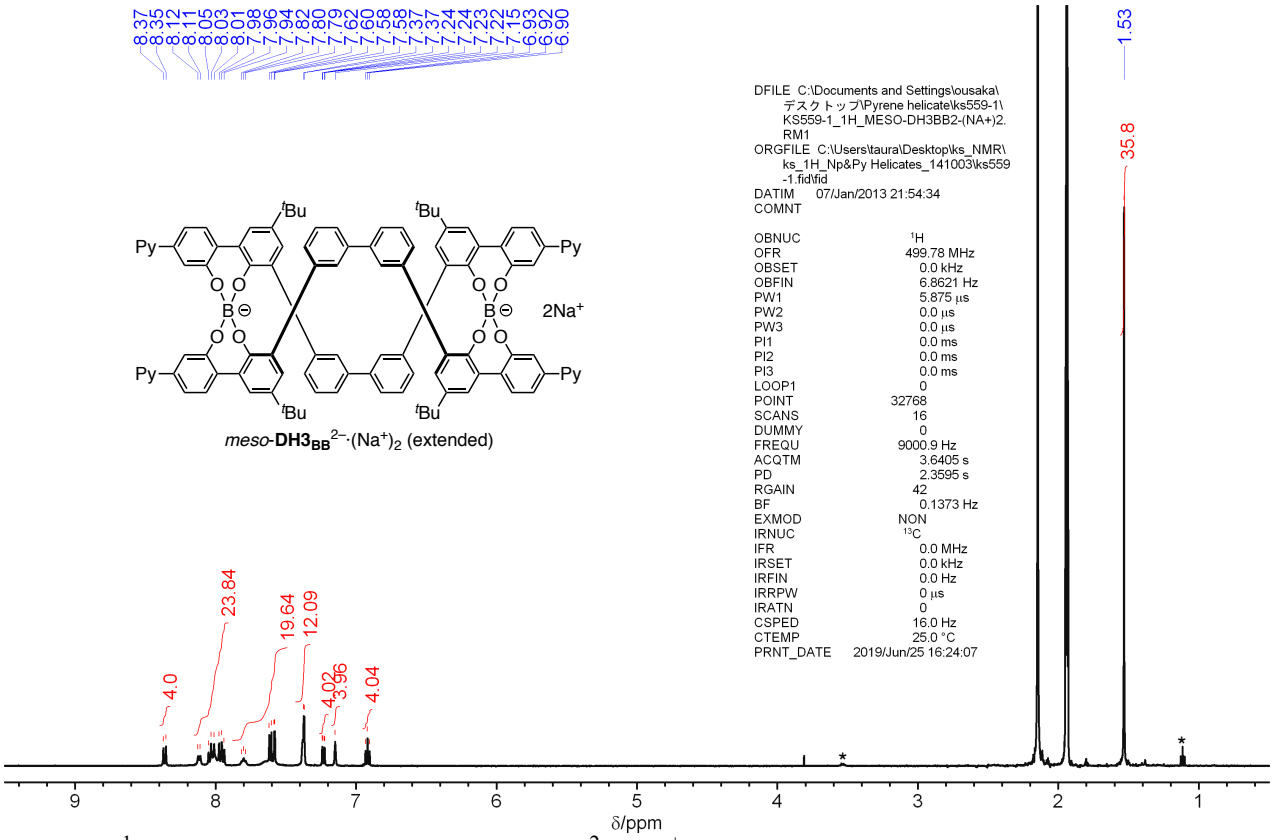

Fig. S23 ^{1}H NMR spectrum of *meso*-$\mathbf{DH3_{BB}}^{2-}\cdot(Na^{+})_2$ in CD_3CN at 25 ºC. * denotes the protons from the residual EtOH used as the solvent.

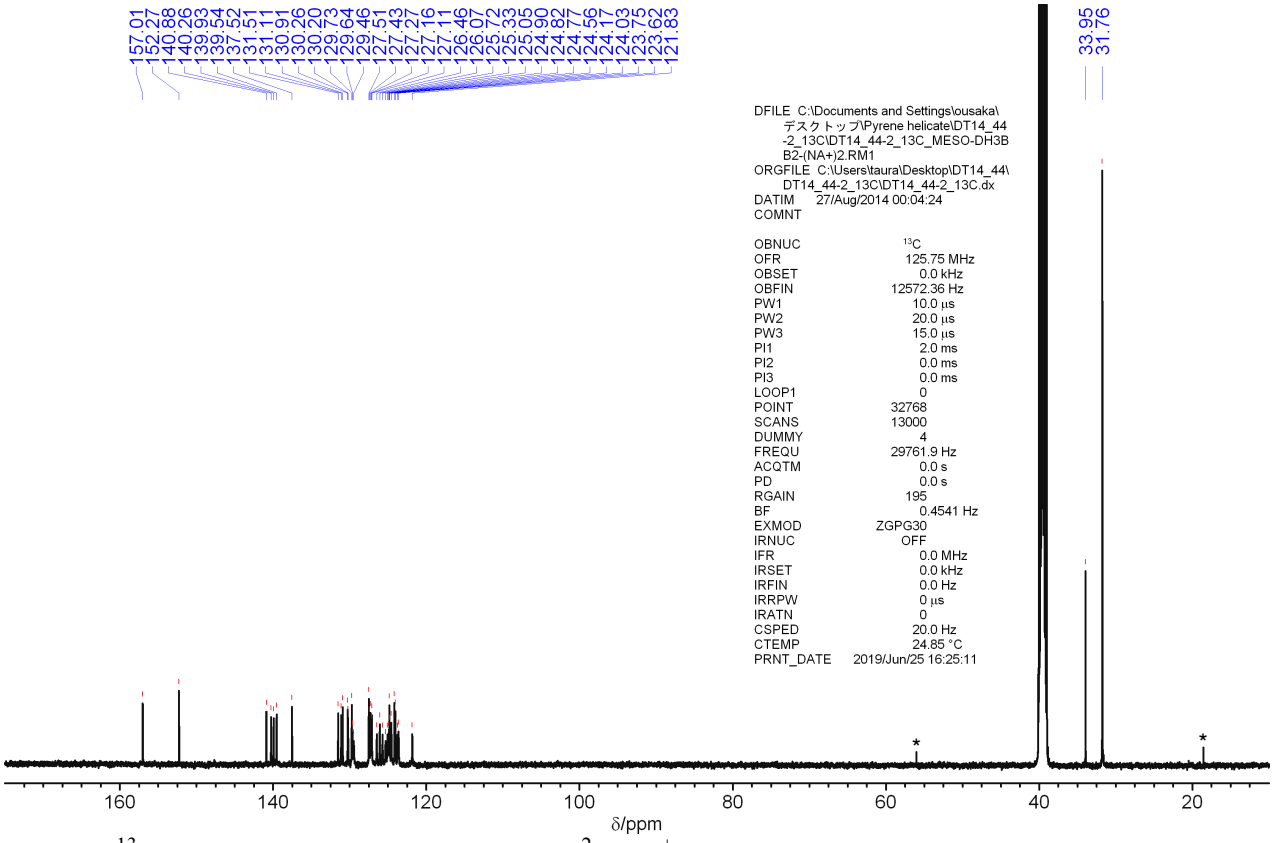

Fig. S24 ^{13}C NMR spectrum of *meso*-$\mathbf{DH3_{BB}}^{2-}\cdot(Na^{+})_2$ in DMSO-d_6 at 25 ºC. * denotes the carbons from the residual EtOH used as the solvent.

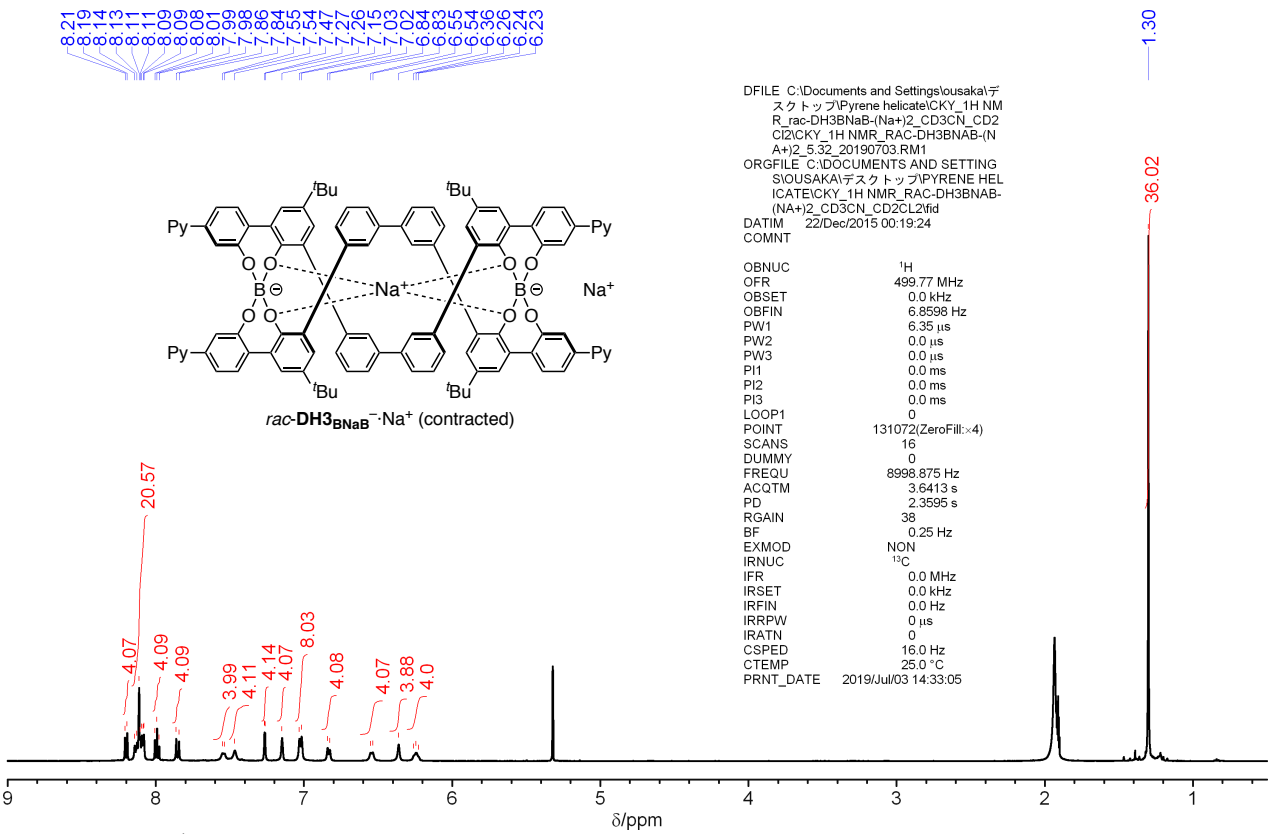

Fig. S25 ^{1}H NMR spectrum of *rac*-**DH3$_{BNaB}$**$^{-}$·Na^{+} in CD_2Cl_2/CD_3CN = 3/1 (v/v) at 25 ºC.

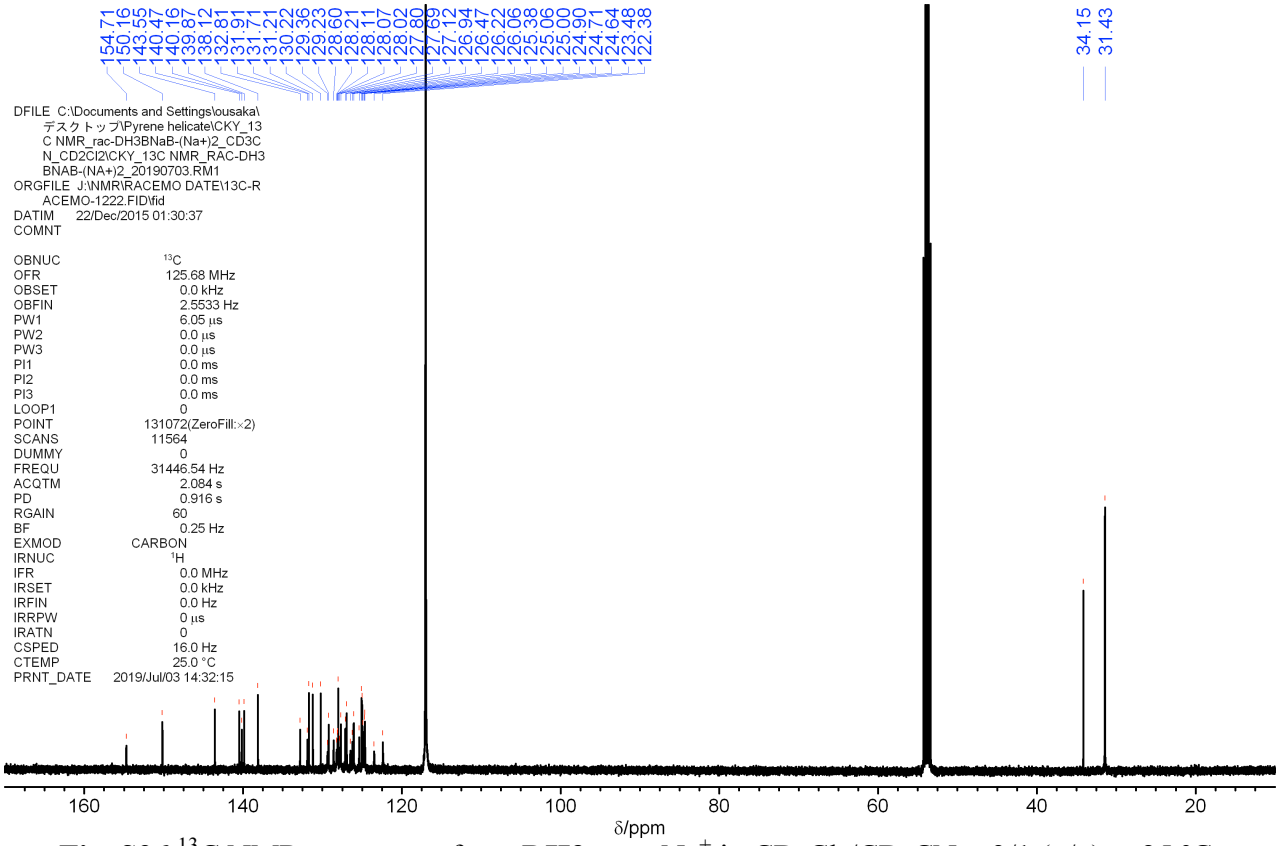

Fig. S26 ^{13}C NMR spectrum of *rac*-**DH3$_{BNaB}$**$^{-}$·Na^{+} in CD_2Cl_2/CD_3CN = 3/1 (v/v) at 25 ºC.